16-000389

59094

BARIUM TRANSPORT AT S-SITE

and

LASER-INDUCED BREAKDOWN SPECTROSCOPY (LIBS)
ITS APPLICATION TO FIELD SCREENING OF BARIUM IN SOILS

Rebecca Ann Brown
Graduate Research Assistant

Group CLS-DO
Brad Martin, Project Leader
OU 1082

Don Hickmott, Ph.D.
Project Geologist

3538

ABSTRACT

The transport of barium in the environment was investigated in this study. Barium has low to very low mobility in most Eh and pH conditions, and will mostly be found adsorbed onto soils due to its high distribution coefficient. Soil samples collected downslope for a barium nitrate storage area showed a peak in barium concentration 120 feet downslope of the source. This could be explained by a slug input of barium into the channel. Aluminum shows the same peak 120 feet downslope from the source, indicating a correlation between barium and aluminum. SEM images show barium in three forms: With sulfate in barite crystals, as a barium compound within feldspar crystals and the pumice matrix, and as a barium compound adsorbed onto organic material.

The use of Laser-Induced Breakdown Spectroscopy (LIBS) to detect barium in soils, thus far, shows a 10.4% relative precision error, but the accuracy and detection limits of the instrument have not yet been determined. Spiked barium sand and soil samples exhibit higher barium to silica ratios because the barium compound exists as a coating on the sample, and is not adsorbed onto the clays and organic matter in the soil.

TABLE OF CONTENTS

CHAPTER 1: Introduction 1
CHAPTER 2: Characteristics of Barium 2
- Chemical 2
- Biological 3
- Regulatory Limits and Detection Limits 4
- Background Barium Levels 4
- Hydrogeochemical 4
- Existing barium data at S-site 6
- Conclusions 9

CHAPTER 3: Barium in Sediments; XRF and SEM Results 11
- Soil Sampling 11
  - Soil Sampling Results 13
  - Discussion 13
- Scanning Electron Microscope 16
  - Barite 16
  - Barium compound 17
  - Barium on organic particles 20
- Conclusions 26

CHAPTER 4: Field Screening for Barium using LIBS 27
- Introduction 27
  - Chromium Study 28
  - Application of LIBS to barium 28
- Methods and Discussion 28
  - Apparatus 28
  - Barium emission lines 30
  - Analysis method 31
  - Spiked sand samples 31
  - Soil samples 33
- Conclusions 36

CHAPTER 5: Further Studies for Barium Transport Project 37
- Soil Samples 37
- LIBS 37

REFERENCES 38
APPENDIX A: Field Soil Sampling 40
- Barium storage/burial site 40
- MDA-P site 41
- Hypalon pond site 42

LIST OF TABLES

Table 2.1: Common barium compounds and their solubilties....2
Table 2.2: Distribution coefficients for barium (MEPAS)....5
Table 2.3: Barium concentrations in soil and water from Turner....6
Table 2.4: Barium concentrations in soil and water from Barr....9
Table 3.1: Soil sampling results....14
Table 4.1: LIBS calibration curve points....35
Table 4.2: XRF powdered standards....35

LIST OF FIGURES

Figure 2.1: Sampling locations in Turner study....7
Figure 2.2: Sampling locations in Barr study....8
Figure 3.1a: Soil sampling locations....12
Figure 3.1: Barium concentration vs. distance....15
Figure 3.2: Barium and aluminum concentration vs. distance....16
Figure 3.3: Barite crystal; MDAP-2....17
Figure 3.4: Barite crystal in organic particle; BBG-4....18
Figure 3.5: EDS spectra of barite....18
Figure 3.6: EDS spectra of barium compound....19
Figure 3.7: Barium compound fragments in pumice matrix; MDAP-2....19
Figure 3.8: Barium compound within feldspar crystal; MDAP-2....20
Figure 3.9a: Barium-rich organic particle; BBG-4....21
Figure 3.9b: EDS spectra of barium compound in organic particle....21
Figure 3.9c: X-ray map of organic particle in figure 3.9a....22
Figure 3.9d: Barite in organic particle....22
Figure 3.10a: Organic particle; BBG-4....23
Figure 3.10b: X-ray map of organic particle in figure 3.10a....23
Figure 3.11a: Barium-rich organic particle; MDAP-2....24
Figure 3.11b: X-ray map of organic particle in figure 3.11a....25
Figure 3.12: Organic particle replaced with barite and barium compound....25
Figure 4.1: LIBS apparatus set-up....29
Figure 4.2: Spectrograph with barium and silica lines....32

CHAPTER 1
Introduction

Barium is a common soil contaminant at Los Alamos National Laboratory's S-site. It is used in the nitrate form, in combination with TNT in a 60/40 ratio, to make a high explosive called Baritol. When Baritol degrades naturally or is burned, barium is left as a residue. There are several places at S-site where barium has been sited as a problem, including an area where barium nitrate was stored unprotected for a period of years, an area where equipment contaminated with HE is burned and then dumped into a landfill, and another area where barium residue, along with other constituents, was collected in a hypalon-lined settling pond.

At this time little is know about the behavior of barium in the environment. To characterize the interaction of barium with soils and water, some key questions need to be answered, including:

1. Will the barium likely be found within surface and groundwater, or within soils and rocks?
2. In what chemical form will barium exist in soils and water?
3. What is the transport mechanism of barium?
4. How toxic is barium in the environment?
5. What are the regulatory limits for barium in soil and water?

This summer the CLS Division of Los Alamos National Laboratory has supported this study to characterize barium transport within soils, surface water, and groundwater at S-site. The other goal of this study has been to determine the viability of using Laser Induced Breakdown Spectroscopy (LIBS) as an inexpensive field screening technique for barium.

This paper is divided into five chapters. Chapter 1 is an introduction to the project, and chapter 2 describes the characteristics of barium, including chemical and biological, regulatory and detection limits, hydrogeological characteristics, and describes two previous studies done on barium at S-site. Chapter 3 describes the findings from this study on barium in sediments, including XRF and SEM results. Chapter 4 describes the LIBS application to barium, and chapter 5 describes some further studies that are recommended for this project.

CHAPTER 2
Characteristics of Barium

Chemical

Barium is a silver-white alkaline earth metal, having similar properties to calcium except that barium is more reactive and has a larger ionic radius. The atomic weight of barium is 137.33 g/mol, and it has seven naturally occurring isotopes. The melting point of pure barium is 729°C and the boiling point is 1,640°C (Chang, 1981). Barium occurs in nature only in a combined state, and its compounds occur in small but widely distributed amounts in the earth's crust (ICAIR, 1990). Barium is divalent and combines readily with oxygen, nitrogen, hydrogen, ammonia, water, halogens and sulfides (Pidgeon, 1964). It occurs most abundantly as sulfate, $BaSO_4$ (barite), and in much smaller amounts as carbonate, $BaCO_3$ (witherite). Barium, as a metal, oxidizes very easily and is decomposed by water or alcohol (CRC, 1086). Substitution of barium for strontium and potassium ions is common. The solubility of barium compounds increases as the pH is decreased. Some common compounds of barium likely to be in the environment are listed in Table 2.1. (CRC, 1986)

TABLE 2.1

Common barium compounds and their solubilities

Barium Compound	Solubility
Barium hexaboride (BaB_6)	Insoluble in cold water
Barium carbonate ($BaCO_3$)	0.002 g/100 ml @ 20°C
Barium chloride ($BaCl_2$)	37.5 g/100 ml @ 26°C
Barium hydroxide ($Ba(OH)_2$)	5.6 g/100 ml @ 15°C
Barium nitrate ($BaNO_3$)	8.7 g/100 ml @ 20°C
Barium oxide (BaO)	8.7 g/100 ml @ 20°C
Barium orthotriphosphate ($Ba_3(PO_4)_2$)	Insoluble
Other barium phosphates	Somewhat insoluble or decompose
Barium selenate ($BaSeO_4$)	0.0118 g/100 ml in cold water
Barium silicate ($BaSiO_2$) (metasilicate)	Insoluble in cold water
Barium sulfate ($BaSO_4$)	0.0002 g/100 ml @ 15°C

In weathering environments of oxidizing and neutral conditions, and either acidic or alkaline pH, barium has low mobility, and in reducing conditions barium has very low mobility (Kabata-Pendias, 1984). The behavior of barium and other trace elements in various weathering environments depends on the stability of the host minerals and on the electrochemical properties of the elements. At S-site barium is in the form of barium nitrate, which is highly soluble, however the burned HE barium byproducts are not known. They could still be barium nitrate, or some other barium compounds which have a different solubility than barium nitrate. Thus the mobility of barium at S-site will depend on what the burned barium byproducts are, and the electrochemical properties of barium. The "electrochemical nature" of an element reflects mainly its electronegativity and its ionic size (Kabata-Pendias, 1984). Elements with ionic potential (ratio of charge to ionic radius) below 3 predominate as free ions in solution, while elements with ionic potential between 3 and 12 tend to form hydrolysates or complex ions. Barium has an ionic potential of 1.3 and thus will be found in solution as a free ion rather than hydrolysates or complex ions (Kabata-Pendias et al., 1984). Ionic barium has a higher electropotential than hydrolysated or complexed barium, and thus will have a greater affinity for association with major elements in soils. This binds the barium to the soil and decreases its mobility in the environment.

Biological

Barium is not an essential nutrient for most biological species. As an environmental pollutant it is moderately toxic. All barium compounds that are water soluble or acid soluble are poisonous (CRC, 1986). It is toxic to humans chemically if it is taken into the body as a soluble salt (i.e. $BaCl_2$). This causes serious deterioration to the heart's function and causes ventricular fibrillations (Chang, 1981). Chronic effects of barium compounds may include bronchial irritation, degeneration of the central nervous system, and damage to the spleen, liver, and bone marrow (ICAIR, 1990). However, if it is ingested as an insoluble sulfate ($BaSO_4$), it can be used as an opaque solution for x-ray studies. The insoluble sulfate is not harmful because the barium is not released directly into the body.

Plants have been shown to accumulate barium from the soil. Thus, food is typically the primary source of barium exposure for the general population (Reeves, 1979). It is also present in seawater, fresh water and municipal waters (ICAIR, 1990).

Barium is emitted into the atmosphere mainly by the industrial processes involved in the mining, refining and production of barium and barium-based chemicals and as a result of combustion of coal and oil (ICAIR, 1990).

Regulatory Limits and Detection Limits

The US Environmental Protection Act (USEPA) drinking water standard for barium is 1 mg/l (1 ppm) (1988). The Subpart S action level is 4000 ppm for barium in soil, and 100 ppm in water. The common detection limit for soil is 10 ppm and for water is 1 ppm, but is dependent on analytical technique.

Background Barium Levels

A study was done in 1979 by Ferendagh, (et. al.) on the soils of Sigma Mesa, a mesa within Los Alamos area. Forty samples of soil were taken and major and minor elements were analyzed. Barium showed a mean concentration of 410 ppm, with a standard deviation of 220. The maximum concentration was 810 ppm and the minimum was 120 ppm. These are assumed to be typical background concentrations of barium within the soil at the lab.

Hydrogeochemical

The principle mineral form of barium is barite which is found in beds or masses of limestone, dolomite, shale and other sedimentary formations. Barium is also present in igneous rocks and coal. A likely control over the concentration of barium in natural surface and groundwater is the concentration of sulfate, which will immobilize the barium ions into the precipitate form (barite). Therefore, under conditions of equal or greater sulfate to barium ratios, the solubility of barite will control the concentration of barium in the natural water.

The distribution of barium between the soil and water phases will be controlled by its distribution coefficient. A distribution coefficient (K_d) is a measure of the affinity of a solute for a solid phase. The higher the K_d value, the greater the tendency of the solute to be sorbed by the soil. K_d is expressed quantitatively as:

$$K_d = \frac{\partial S}{\partial C}$$

where S = mass of chemical constituent adsorbed on the solid part of the porous medium per unit mass solid, and C = solute concentration in solution.

Two references for distribution coefficients for barium were found. The first is from the Multimedia Environmental Pollutant and Assessment System (MEPAS) Constituent Data Base, which gives a range of K_d (in mg/l) for barium (Table 2.2) for three different pH values and soil compositions (total weight percentage of clay, organic matter, and iron and aluminum hydroxides).

The second source for barium K_d comes from a report from the University of Waterloo on barium and radium migration in unconsolidated Canadian geological materials (Gillham, 1981). This report describes the laboratory studies of distribution coefficients for barium in geologic materials varying from coarse sand to clayey loam. The K_d values ranged between 60 and 3,500 mg/l and appear to be influenced by the amount of barium occurring naturally in the soil materials.

TABLE 2.2

Distribution coefficients for barium (MEPAS)

	< 10%	10 - 30%	> 30%
pH ≥ 9	530	2800	16000
pH 5 - 9	530	2800	16000
pH ≤ 5	53	280	1600

The distribution coefficient is important in determining the retardation of an element within a solid phase, as described by the Retardation Equation:

$$\frac{v}{v_c} = 1 + \frac{r_b}{n} \cdot K_d$$

where v = average linear velocity of groundwater, v_c = velocity of the retarded constituent, r_b = dry bulk density of solid phase, and n = porosity of solid phase (Drever, 1988). The expression $\{1+ (r_b/n) \cdot K_d\}$ is called the Retardation Factor. Dry bulk density (r_b) for unconsolidated sediments is typically around 2.65, and porosity (n) for unconsolidated sediments ranges from 0.2 to 0.4. Thus the (r_b/n) ratio ranges from 4 to 10 for unconsolidated sediments. If an element has a K_d value of 1, the solute will be retarded by a factor of 5 to 11. If K_d values are orders of magnitude larger than 1, the solute is essentially immobile. So the barium K_d values of 53 to 16,000 suggest that barium is essentially immobile in the water phase and is strongly attracted to the solid phase (i.e. soils and rock), although, given the wide range of K_ds, it is clear that many different factors are involved.

Existing barium data at S-site

Two small-scale studies have been done to delineate the HE and barium contamination problems at S-site. The first study was by Turner (1971), which sampled water and soils for RDX-HMX (high explosives), barium, TNT, and boron. The soil and water samples were taken from the drainage floor of Water Canyon and Del Valle Canyon, and water samples were taken from the outlets of settling basins adjacent to operating buildings (figure 2.1). Significant results for barium are presented in Table 2.3. The soil barium analyses were done on residual water from the soil and not on the soil itself. Therefore the soil samples show very low barium concentrations.

TABLE 2.3

Barium concentrations in soil and water from Turner study

Sample Location	Ba Concentration
Water sample from settling tank behind Bldg. 260	4 ppm
Soil sample from the natural drainage area for the MDA-P burning pit	14 ppm
Water canyon	None
Along Del Valle Canyon:	
Water sample of surface drainage from Bldg. 260	30 ppm
Soil sample 400 yds down from Bldg. 260	9 ppm
Soil sample 100 yds down from previous	3 ppm
Water sample 100 yds down from previous	1 ppm
Water sample taken from point where drainage from MDA-P hits the canyon floor	27 ppm
Water sample taken 100 yds down from previous	15 ppm
Water sample taken 100 yds down from previous	8 ppm
Water sample taken 100 yds down from previous (water in pool)	11 ppm
Soil samples downstream from previous to the confluence of Del Valle and Water Canyon	Positive but not quantitatively detectable

The second study done on barium characterization at S-site was described by Mike Barr from WX-3 in an interview on 6/1/92. This was a limited study done for MDA-R

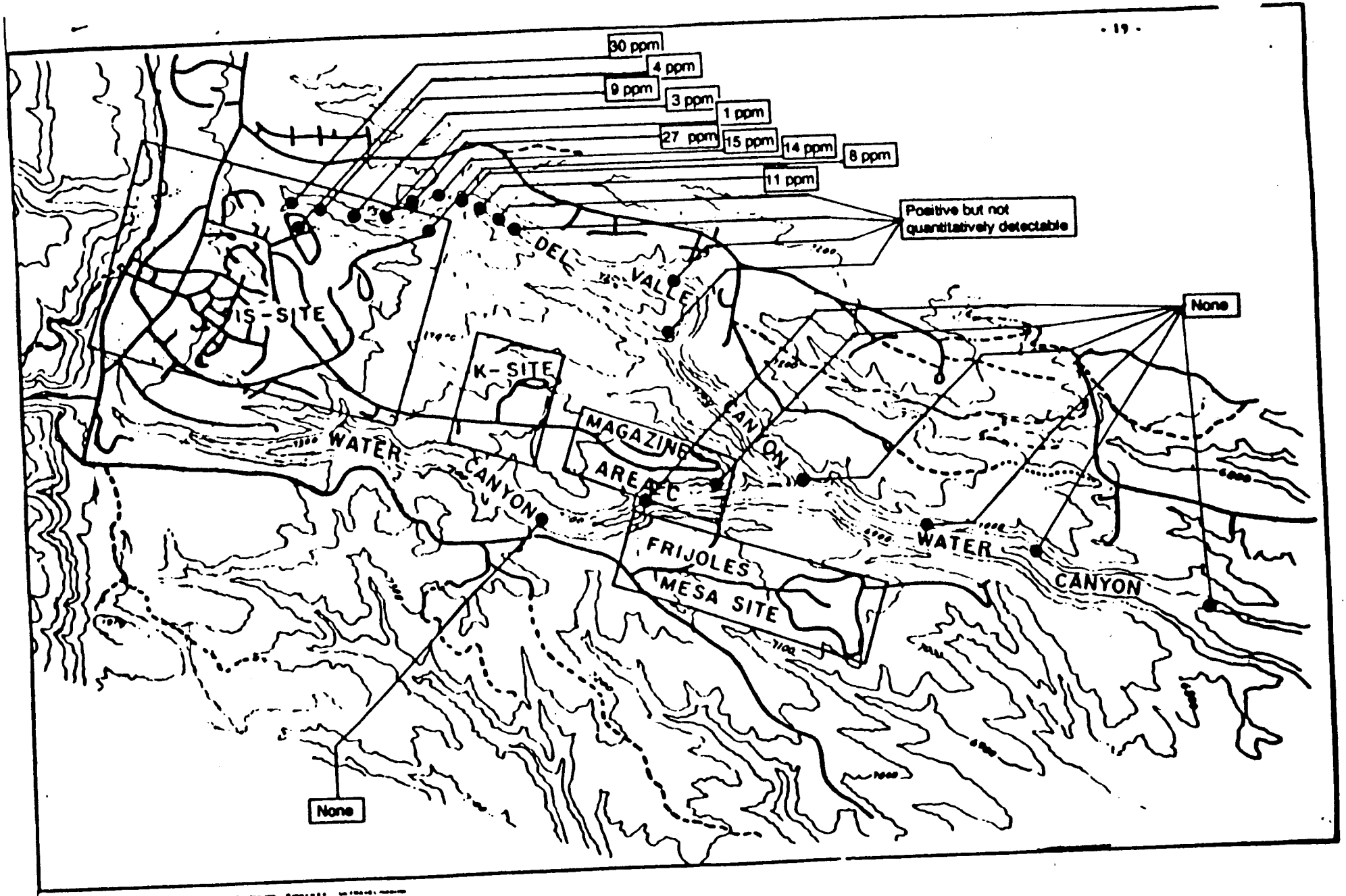

Figure 2.1: Sampling Locations in Turner Study

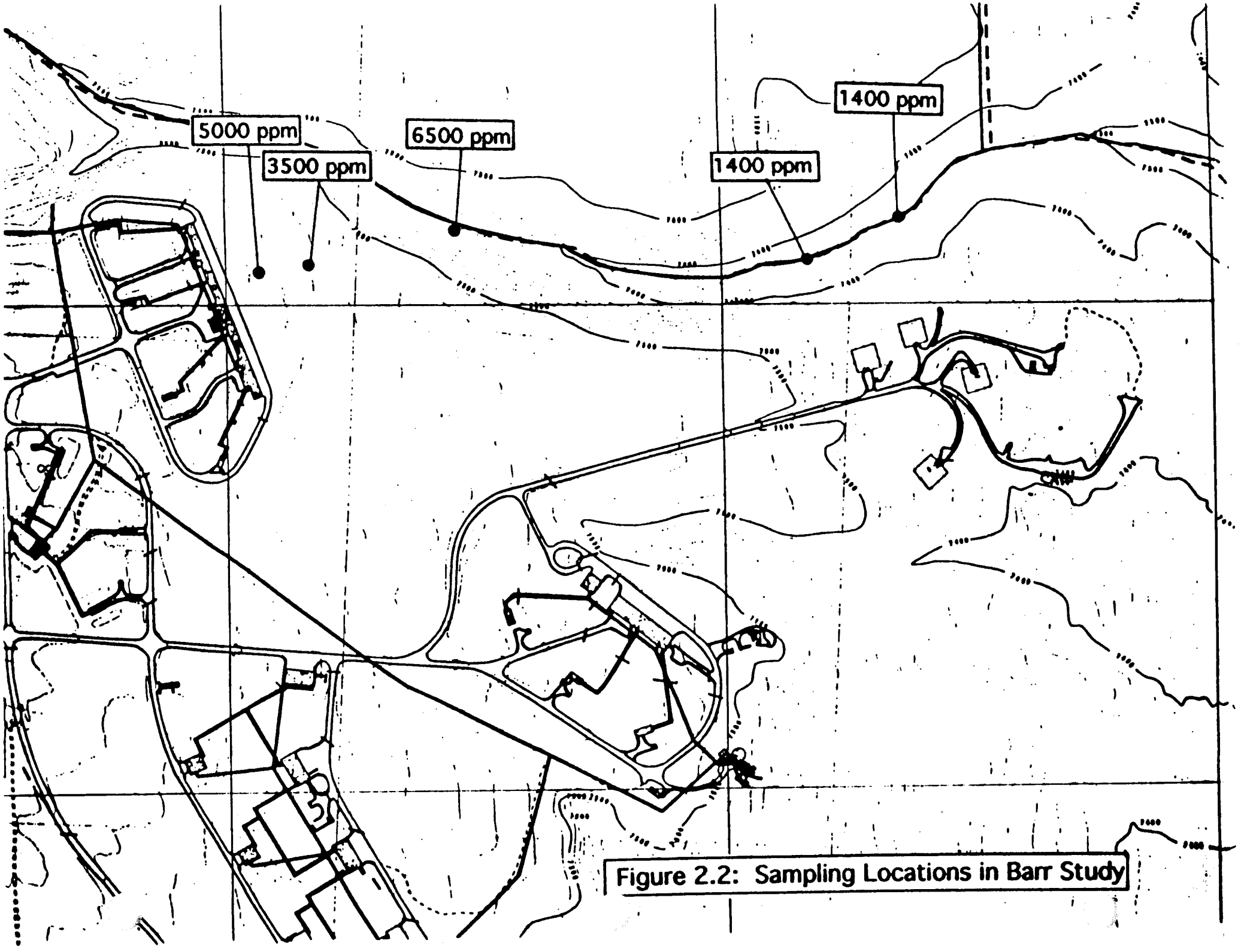

Figure 2.2: Sampling Locations in Barr Study

and MDA-P (behind Bldg. 260 and the burning ground/landfill site respectively) (see figure 2.2). Mike describes MDA-R as an area where streams begin and eventually converge into one stream which runs by MDA-P. Wet soil samples in stream beds were taken and ranged from 0.1% by weight Ba up to 0.85% Ba (1000 ppm to 8500 ppm Ba). Results are presented in Table 2.4.

TABLE 2.4

Barium concentrations in soil and water from Barr study

Sample Location	Ba Concentration
Pond behind Bldg. 260	5000 ppm (with a high amount of HE)
Downstream of this pond 135 ft.	3500 ppm
210 ft. downstream - natural ponding area	6500 ppm
Area P burning ground (above)	1400 ppm
Area P burning ground (below)	1400 ppm

The Barr findings on barium concentrations within S-site suggest a high level of barium contamination behind building 260 , but only a small problem within Del Valle Canyon. The Turner study shows very low concentrations of barium within soil water and surface water samples. This is expected due to the high distribution coefficient of barium, where most barium will be adsorbed onto clay and organic matter particles, and very little will exist in solution.

Conclusions

1. Barium occurs most abundantly as sulfate, $BaSO_4$ (barite) and in smaller amounts as carbonate, $BaCO_3$ (witherite).
2. Barium has low mobility in oxidizing and neutral conditions, either alkaline or acidic pH, and very low mobility in reducing conditions.
3. Barium will be found in solution as a free ion rather than hydrolysate or complex ion.
4. Barium is toxic to humans if taken into the body as a soluble salt, but as an insoluble sulfate it is used as an opaque solution in X-ray studies.
5. The Subpart S action level for barium is 4000 ppm in soil and 100 ppm in water.

6. Barium has a very high distribution coefficient, and therefore will be highly adsorbed onto soils. The distribution coefficient depends on soil pH and clay, iron and aluminum oxide, and organic matter content in the soil.

CHAPTER 3
Barium in Sediments
XRF and SEM Results

Soil Sampling

Soil samples were taken from three different locations at S-site. The locations were suspected to have high barium and low HE concentrations. Figure 3.1a shows the soil sampling locations. Each sampling location is described in detail in Appendix A.

The first group of samples taken were downslope of a barium nitrate storage area at the TA-16 burning ground, northeast of site 16-386. In the late 1940s this site was used as a barium nitrate storage area and possibly as a landfill. A site worker states that there was a large uncovered barium nitrate pile located within the fenced 386 burn area in 1966. This pile was about two dump truck loads resembling a "large pile of snow." When he returned to the site in the early 1970s the pile was gone. It has been suggested that this pile was either buried at the site (the site is sometimes referred to as the barium nitrate burial ground) or was taken off site. Since then barium nitrate has been stored at the site, but in sealed containers.

Six soil samples were taken from a dry stream bed which runs through the storage area, downgradient from the area, beside MDA-P, and eventually into Del Valle Canyon. Samples were taken to determine the levels of barium coming from the storage area, and to ascertain how far the barium has travelled down the most likely transport path, the stream bed. One sample (BBG-5) was taken beside MDA-P to determine if the landfill (see description below) is contributing barium contamination to this drainage, or if all barium in the drainage is from the storage area. An upslope sample (BBG-6) was taken to determine background barium concentrations within the stream bed soils.

The next group of soil samples were taken from MDA-P (Material Disposal Area- P), an industrial landfill that was used to dispose of residues resulting from the burning of HE contaminated materials such as concrete rubble, tables, bottles, etc.. Barium is expected to be present in the landfill since it contains residua of the burned HE, but levels of HE present in the landfill are uncertain.

Two samples were taken from the canyon side of the landfill from two terraces. The first sample (MDA-P-1) was taken from the first terrace (closest to the top of the landfill) and contained HE levels too high to remove from the site. WX-Division has a field screening technique for determining HE levels in soils, rocks, and water that is

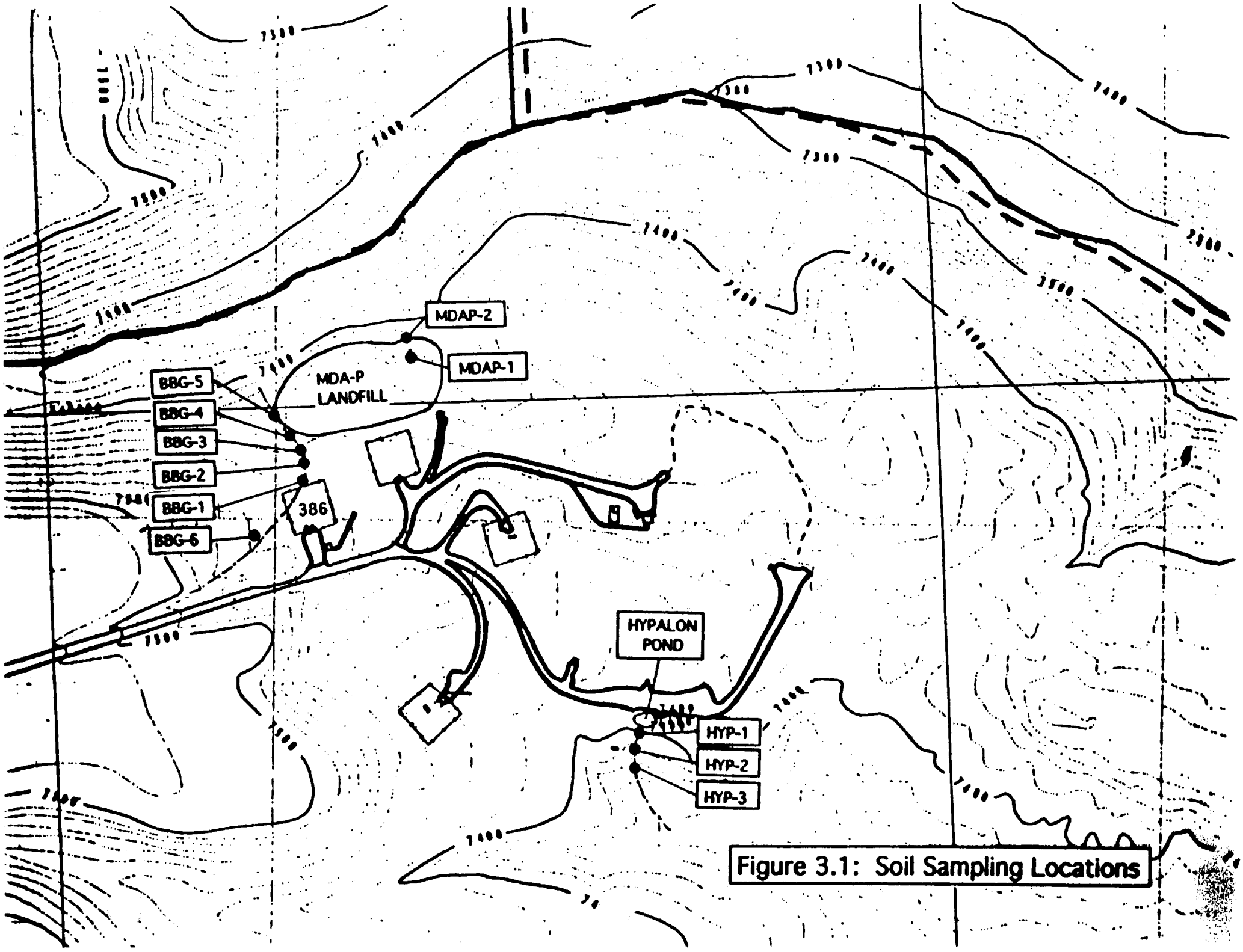

Figure 3.1: Soil Sampling Locations

sensitive to 100 ppm. If a sample fails this test (i.e. has HE levels greater than 100 ppm), the sample is not allowed off of the site. The second soil sample (MDA-P-2) was taken from a terrace further down the slope of the landfill and passed the HE field test.

The third group of samples were taken downslope from a decommissioned hypalon-lined pond located at the TA-16 burning ground. The pond received liquid from two filtration beds to the north of the pond and has historically had high barium levels. Before residual liquid was discharged to an outfall the barium levels were reduced to below 100 ppm by adding sodium sulfate to precipitate out barium sulfate. The receiving canyon for this pond was sampled for barium in 1987. Barium concentrations ranged from 26.2 mg/l at 3 feet below the outfall, to 6.6 mg/l at 10 feet below the outfall, and 2.7 mg/l at 40 feet below the outfall. Local background level was shown to be 0.8 mg/l. Three soil samples were taken from sediment traps in the drainage below the hypalon pond.

Soil Sampling Results

The soil samples were analyzed by X-ray Fluorescence (XRF) , using pellets made of a 50/50 ratio of soil sample to lithium tetraborate binder. Table 3.1 shows the major and minor element concentrations in the soil samples.

Discussion

The BBG samples reveal an interesting trend in barium concentration versus distance from the source (figure 3.1). A linear or exponential decrease in barium concentration from the source was expected, however the samples show a peak in barium concentration 120 feet downstream from the source. The sample closest to the source is elevated relative to background and samples show an increase in concentration until the peak at the BBG-4 sampling location. This sample was taken upgradient from MDA-P, so there is no influence in barium concentration from the landfill. Downgradient from BBG-4 barium concentration decreases. BBG-5 was taken next to MDA-P to see if the landfill was contributing barium to the channel. It is unlikely that a significant amount of barium is being added to the channel at this point because the barium concentration drops significantly from BBG-4 to BBG-5.

There are two possible explanations for the trend in barium concentration downslope from the barium storage area. First, the barium concentration in each sample could be a function of clay, aluminum and iron oxide, or organic matter content in the soil. It was shown in Chapter 2 that barium has a very high distribution coefficient and thus will be strongly adsorbed onto solid particles. The distribution

TABLE 3.1

Soil Sampling Results

Sample	Na2O %	MgO %	Al2O3 %	SiO2 %	P2O5 %	K2O %	CaO %	TiO2 %	MnO %	Fe2O3 %
BBG-1	4.69	0.36	12.99	72.52	0.02	3.69	0.81	0.40	0.07	2.67
BBG-2	4.70	0.37	13.23	69.51	0.01	3.84	0.73	0.60	0.09	3.79
BBG-3	4.44	0.35	13.41	70.63	0.03	3.92	0.71	0.36	0.07	2.76
BBG-4	4.32	0.40	13.91	68.02	0.03	4.09	0.65	0.41	0.05	2.94
BBG-5	4.55	0.37	13.51	70.17	0.03	3.86	0.71	0.37	0.06	2.72
BBG-6	3.23	0.44	12.17	71.30	0.03	3.48	0.86	0.44	0.06	2.08
MDA-P-2	4.07	0.30	12.76	69.08	0.05	4.25	0.60	0.30	0.06	2.22
HYP-1	3.28	0.32	10.50	76.75	0.04	3.33	0.80	0.31	0.05	2.32
HYP-2	4.09	0.39	11.90	74.51	0.05	3.49	0.88	0.31	0.06	2.59
HYP-3	4.39	0.42	13.51	70.14	0.05	4.11	1.24	0.30	0.07	2.58

Sample	V ppm	Cr ppm	Ni ppm	Zn ppm	Pb ppm	Sr ppm	Y ppm	Zr ppm	Nb ppm	Ba ppm
BBG-1	40	8	15	157	56	152	16	373	34	1750
BBG-2	47	10	16	102	61	142	17	534	38	2351
BBG-3	43	8	16	70	71	135	19	320	38	2658
BBG-4	42	7	16	61	88	128	31	412	46	6253
BBG-5	44	8	14	58	73	129	20	326	37	2823
BBG-6	42	14	13	39	93	132	31	406	41	620
MDA-P-2	41	3	19	80	98	134	32	324	49	10026
HYP-1	39	7	15	61	84	143	19	268	32	1430
HYP-2	38	6	14	73	78	137	23	275	38	941
HYP-3	36	7	16	73	103	130	30	304	44	1180

Figure 3.1
Barium Concentration vs. Distance

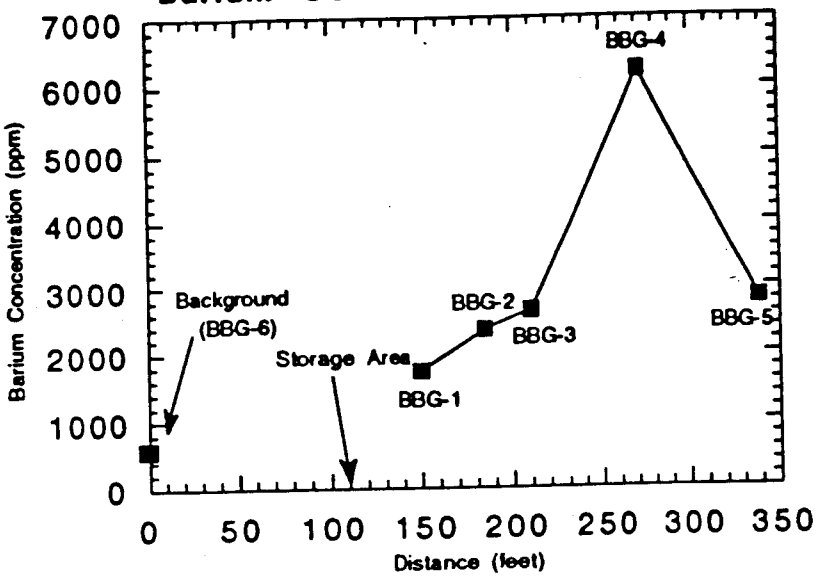

coefficient increases with higher pH and higher percentages of clay, aluminum and iron oxides, and organic matter in the soil. Thus barium concentrations will be higher in soils with increasing percentages of these constituents. If these factors vary downstream, corresponding barium concentrations would also vary. A full soil analysis of the BBG samples, including sand/silt/clay fractions, soil pH, organic matter content, and microprobe analysis of the clays in the soil would help to determine if there is a correlation between these factors and barium content. However, lack of time precluded a full soil analysis for this study. Therefore, in an effort to find some correlation, major element concentrations from the XRF analyses were plotted with barium versus distance. Aluminum shows the most significant correlation with the barium distribution (figure 3.2), with an upward trend from the source to a peak in aluminum concentration at BBG-4, and a decrease in concentration downgradient from there. This aluminum correlation could reflect either a variation in the amount of aluminum oxide or clay percentage in the soils.

A slug input of barium at the storage area is the second possible explanation of the barium trend down the stream bed. At the barium storage ground there was a limited duration of contaminant input while the uncovered barium nitrate pile was stored at the site. Sediments immediately around the pile would have been highly contaminated with barium. Since the pile's removal in the early 1970s the amount of

Figure 3.2
Barium and Aluminum vs. Distance

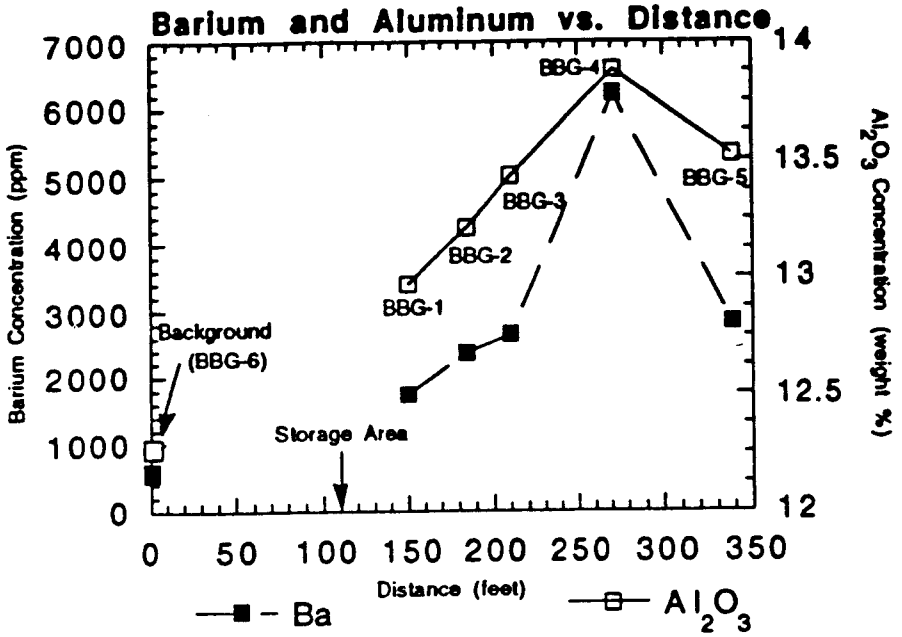

barium input to the sediments has been greatly reduced. The highly contaminated sediments have since moved down the stream bed through yearly rains and snow melt runoff, and sediments behind the contamination peak have been less contaminated. Thus we might expect to see a peak in barium concentration some distance downstream from the source.

Scanning Electron Microscope

Soil samples BBG-4 and MDAP-2 were analyzed using the scanning electron microscope (SEM) to determine where the barium resides within the soil. Five random sites were chosen from the slide of each sample and X-ray maps of barium, sulfur, titanium, and aluminum or iron were made of each site. Barium was found in three different forms throughout the two slides; With sulfur in barite crystals, as an oxide or carbonate within feldspar crystals and the pumice matrix, and as a barium compound adsorbed onto organic material.

Barite

Barite crystals are found in two forms: Within the pumice and feldspar matrix, and in void structures in organic material. The barite crystals are easily detected where the barium and sulfur x-ray maps display high intensities in the same area. Figure 3.3 shows a high magnification view of one barite crystal within the pumice

matrix. The fragment in the lower left hand corner is a pumice fragment, and the surrounding dark areas are void space. Figure 3.4 shows a barite crystal within the pore of an organic particle (see discussion below). Figure 3.5 shows a typical EDS spectra for barite.

Figure 3.3
Barite Crystal; MDAP-2

Barium compound

A barium compound of some kind, perhaps barium oxide, barium carbonate, barium hydroxide, or a barium and iron mixture, is found throughout the pumice and clay matrix and within feldspar crystals. Figure 3.6 shows an EDS spectra from one of these barium fragments, which shows only barium peaks. Since light elements such as oxygen and carbon can not be detected on this SEM, it is unknown at this time the exact composition of this barium compound. Figure 3.7 shows several barium compound fragments (the lighter fragments) within the pumice clay matrix. Figure 3.8 shows barium compound fragments within a feldspar crystal.

Figure 3.4

Barite Crystal in Organic Particle; BBG-4.

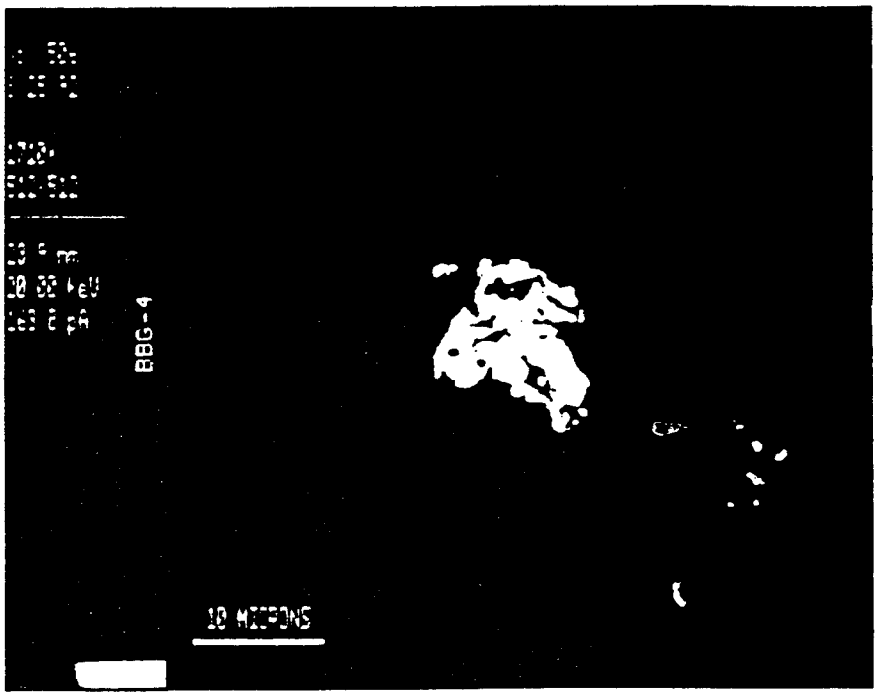

Figure 3.5

EDS Spectra of Barite

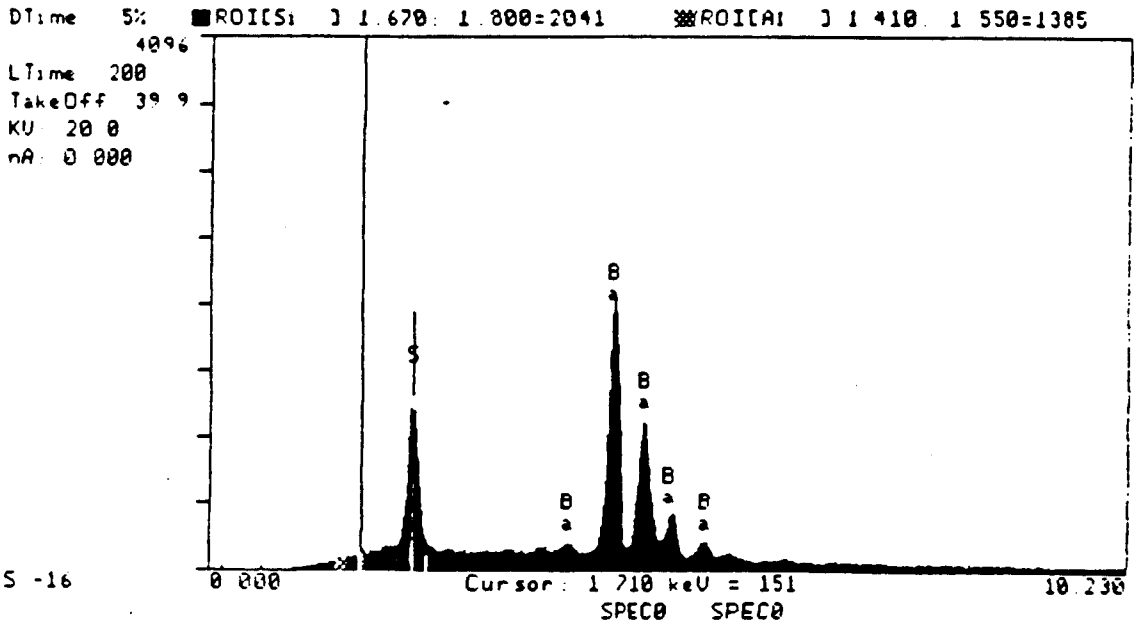

Figure 3.6

EDS Spectra of Barium Compound

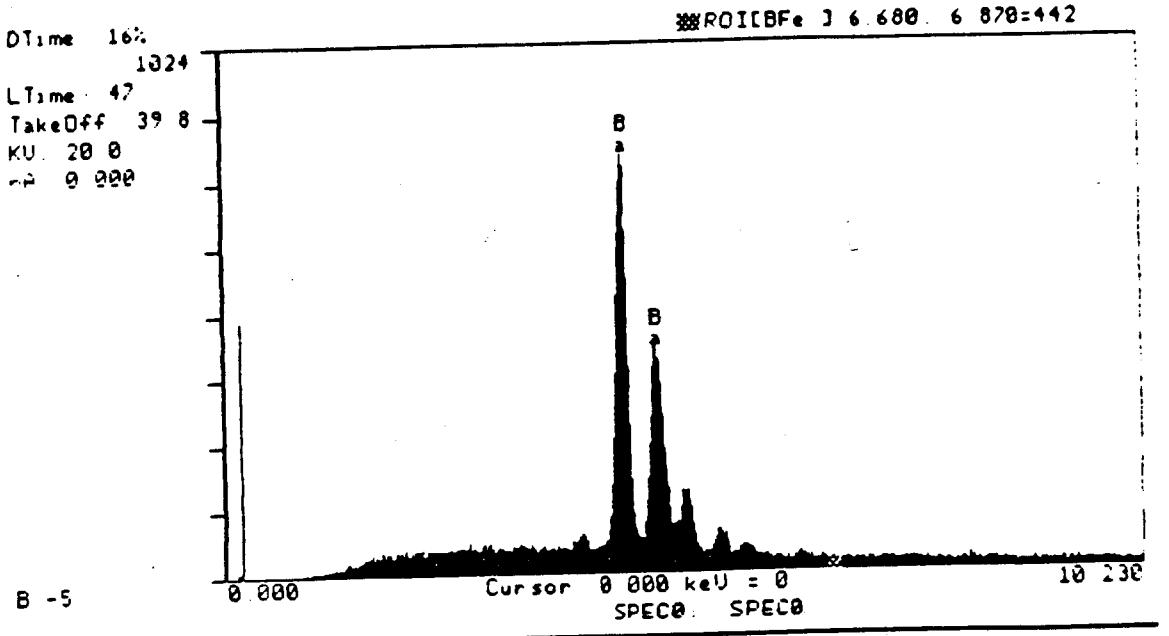

Figure 3.7

Barium Compound Fragments in Pumice Matrix; MDAP-2

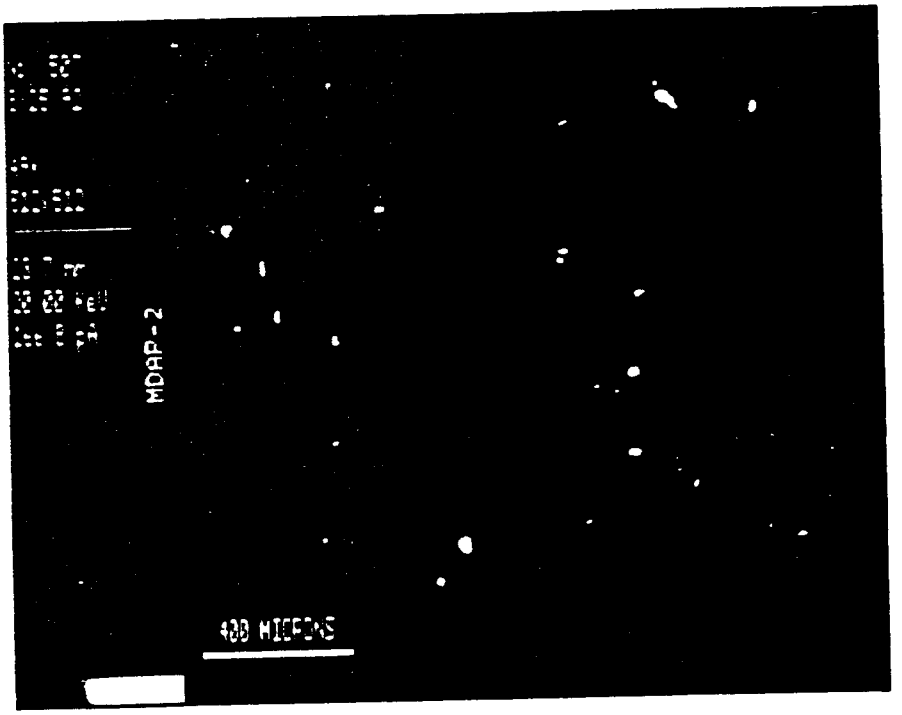

Figure 3.8

Barium Compound within Feldspar Crystal; MDAP-2

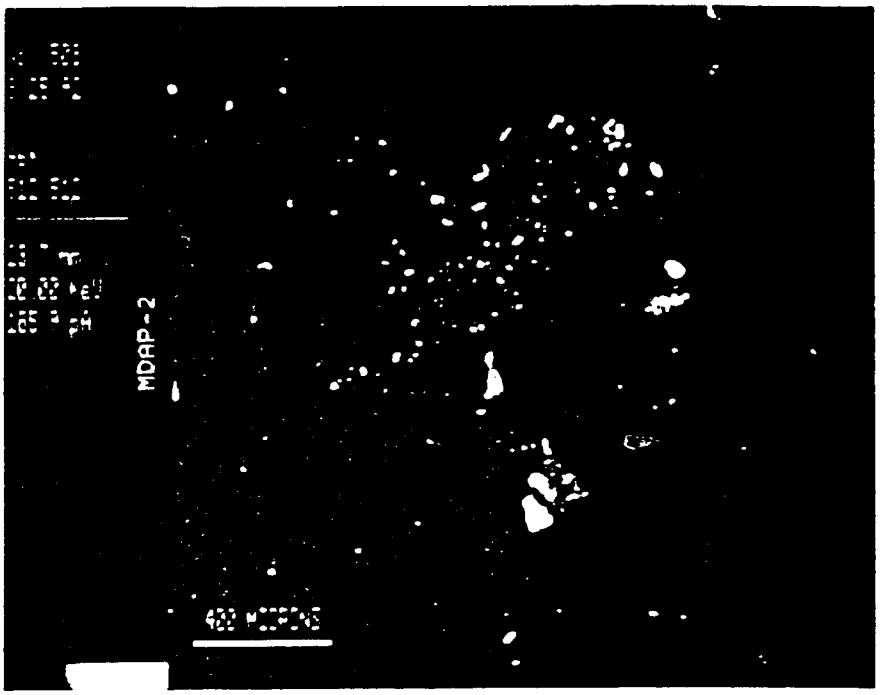

Barium on organic particles

Four organic particles were found on the two slides. Figure 3.9a shows one particle that exhibits regular spaced pores with a definite septum structure in between pores. EDS analysis of the septa structure (figure 3.9b) shows barium and calcium, with no silica, indicating the particle is not a pumice fragment. The pumice fragments found in the soil thin sections do not exhibit regular spacing of pores and are composed mainly of silica. This particle appears to be a transverse cross-section through a piece of wood. The X-ray map of the organic particle (figure 3.9c) shows a marked affinity of barium for the particle with respect to the surrounding matrix. There are a few high intensity spots within the particle which correlate on the barium and sulfur maps. EDS analysis of these spots show both barium and sulfur, so it is likely that these are small barite crystals. Figure 3.4 above showed a barite crystal within a void of this organic particle. It appears that the barite is filling in the pores of the organic particle (figure 3.9d). Figure 3.10a shows another organic particle on the BBG-4 slide. This particle appears to be a longitudinal cross-section through a piece of wood. EDS analysis of the structure walls shows barium and calcium, with no silica, similar to the previous organic particle. The barium X-ray map of this area (figure

Figure 3.9a

Barium-Rich Organic Particle; BBG-4

Figure 3.9b

EDS Spectra of Barium Compound in Organic Particle

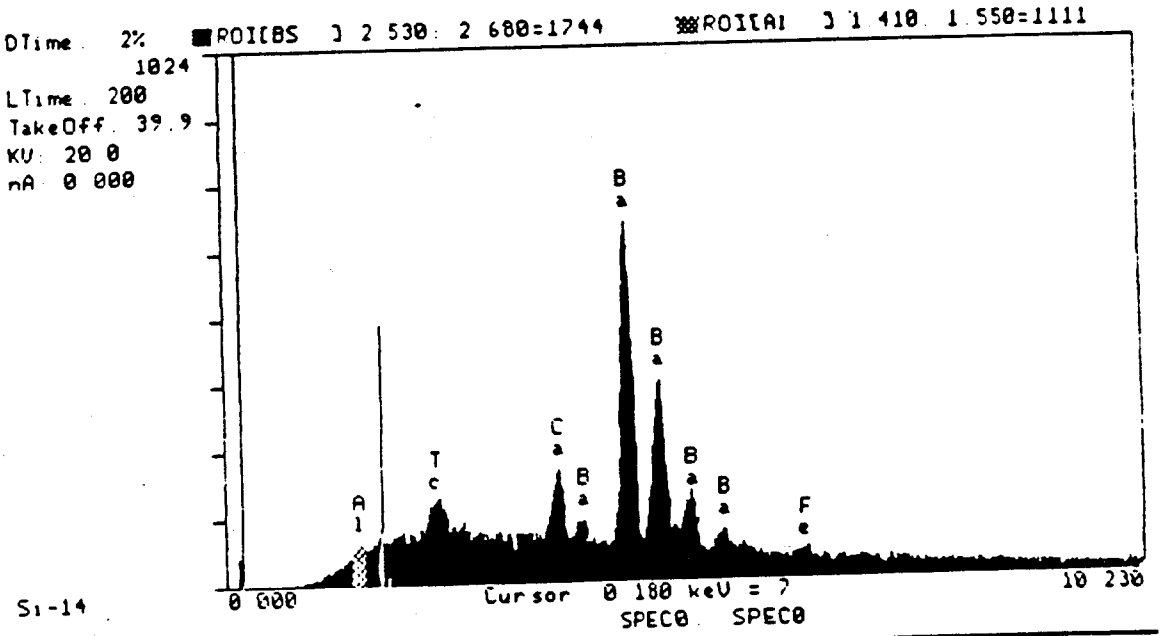

Figure 3.9c

X-ray Map of Organic Particle in Figure 3.9a

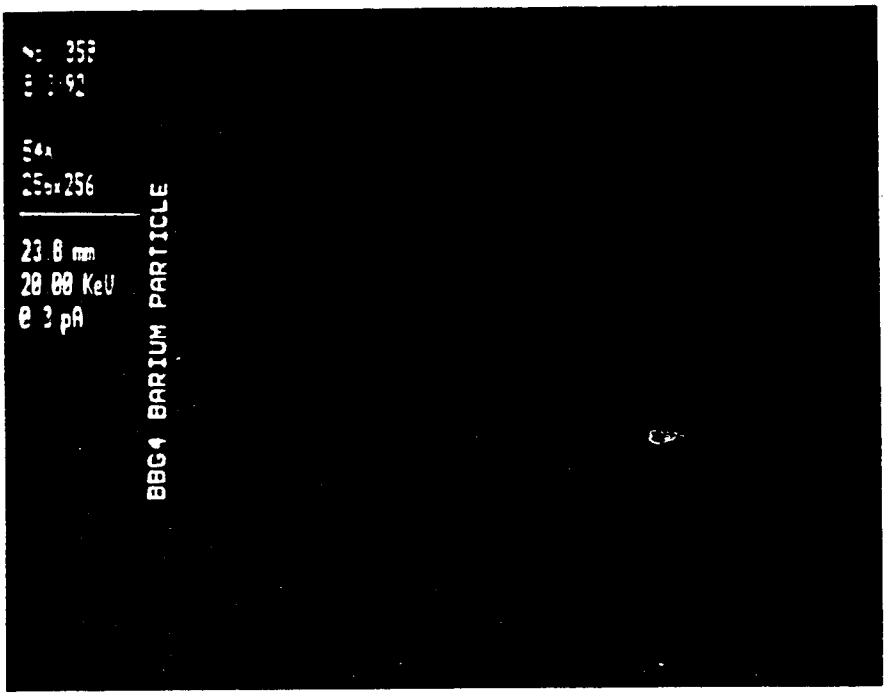

Figure 3.9d

Barite in Organic Particle

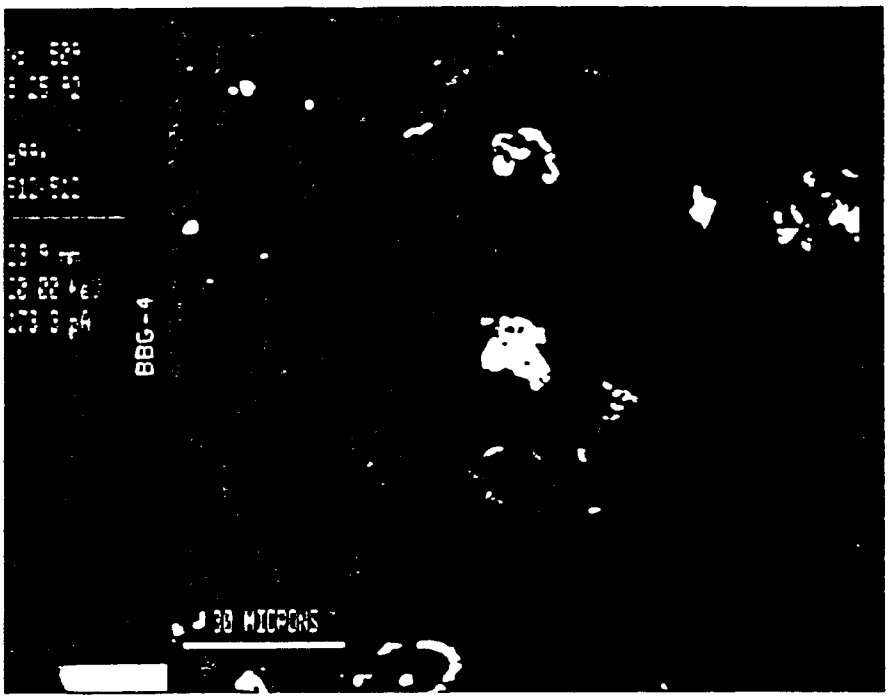

Figure 3.10a

Organic Particle; BBG-4

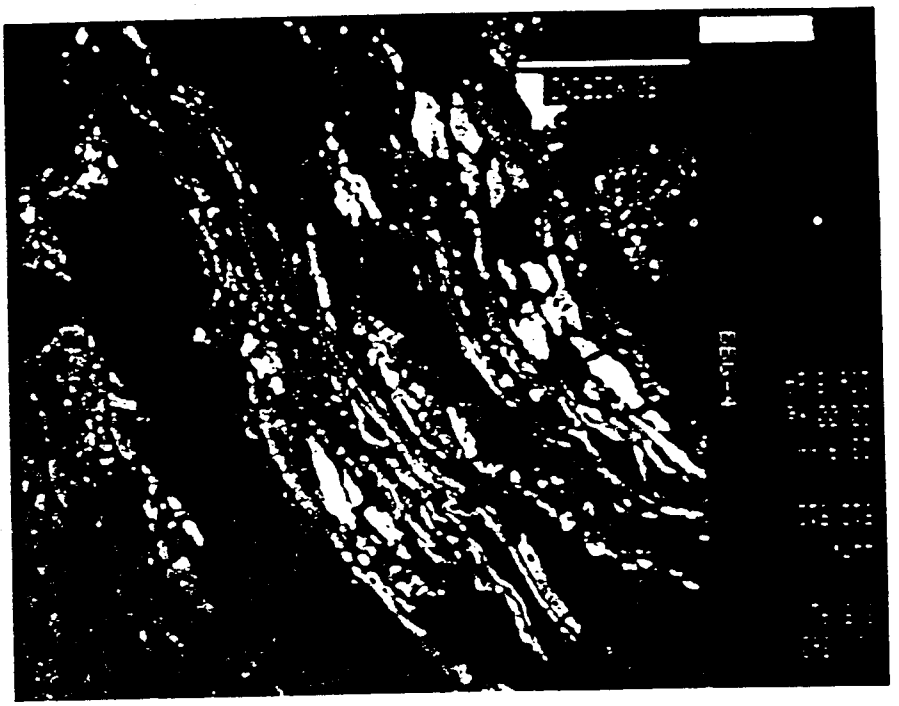

Figure 3.10b

X-ray Map of Organic Particle in Figure 3.10a

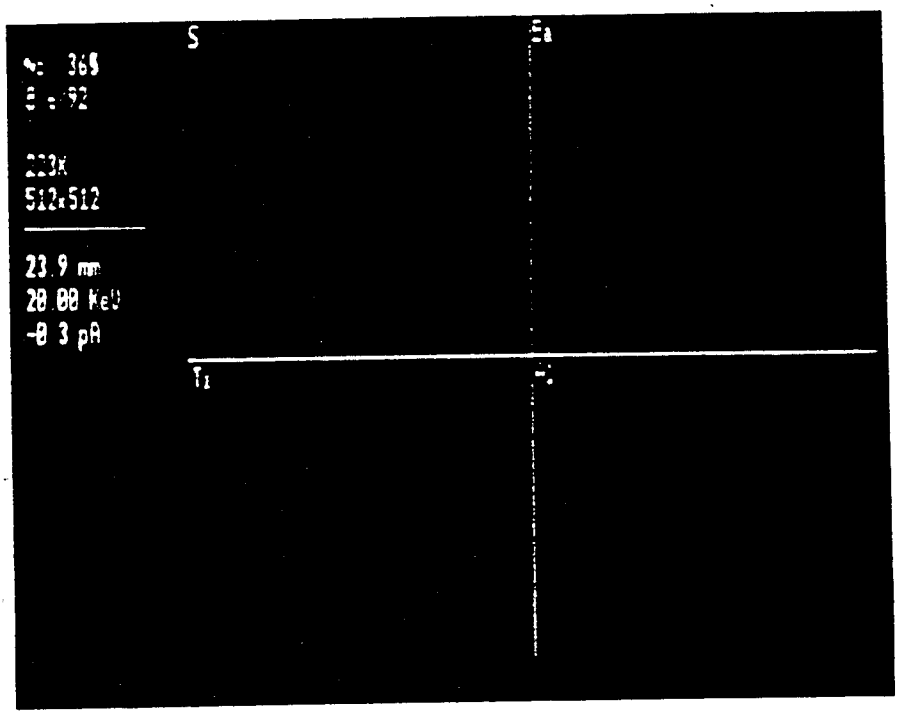

3.10b) closely mirrors the particle structure. A few high intensity areas of barium correlate to sulfur presence on the map, indicating barite growth within the organic particle. Titanium shows a very similar pattern to barium on the map. The titanium and barium peaks are very close together and tend to interfere. The primary barium peak used for the X-ray maps was moved to avoid picking up titanium signal in the X-ray maps. Therefore, most of the signal on the titanium map is barium.

Two barium-rich organic particles were also found in the MDAP-2 slide. The first (figure 3.11a) is a transverse cross-section through a piece of wood, similar to the first organic particle described in BBG-4. The barium X-ray map (figure 3.11b) also shows a high affinity of the barium for the organic particle with respect to the background matrix. The void spaces in this particle are also being filled in with barite and the mystery barium compound described earlier. The other suspect particle on the MDAP-2 slide (figure 3.12) appears to be a longitudinal cross section of a piece of wood which has been highly replaced with barium. Remnant pore structures can be seen in the middle of the particle, while the edges appear to have been nearly completely replaced with barium. EDS analysis of the infilling material shows the typical barium and calcium spectra, with a little bit of barite throughout.

Figure 3.11a

Barium-Rich Organic Particle; MDAP-2

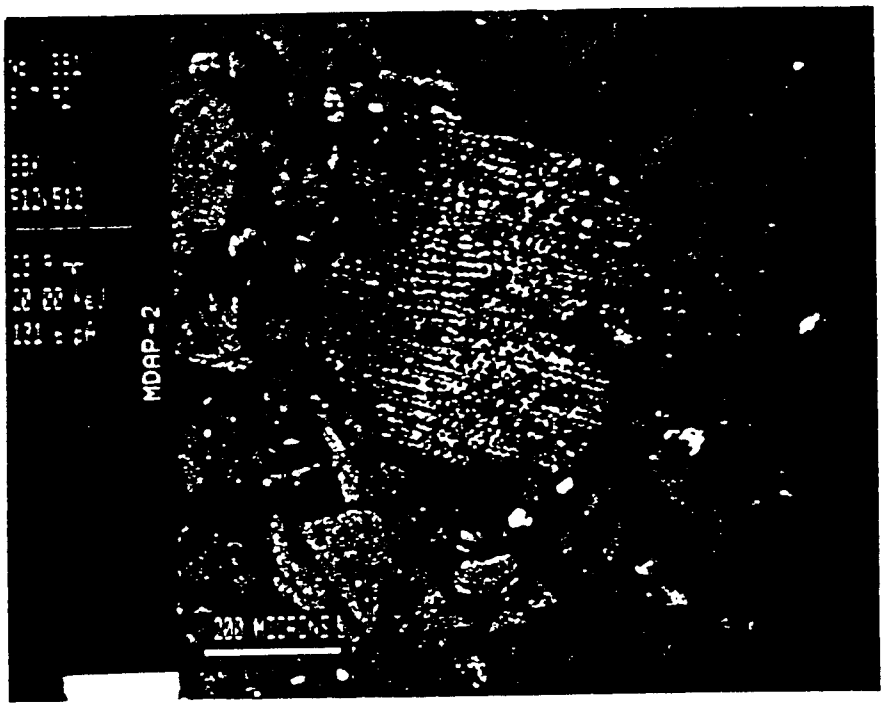

Figure 3.11b

X-ray Map of Organic Particle in Figure 3.11a

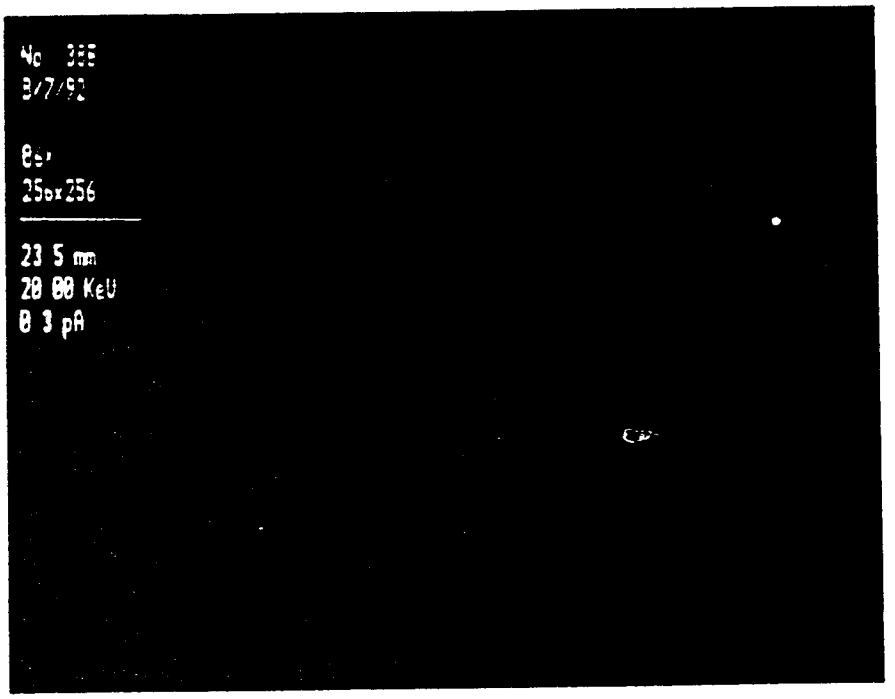

Figure 3.12

Organic Particle Replaced with Barite and Barium Compound; MDAP-2

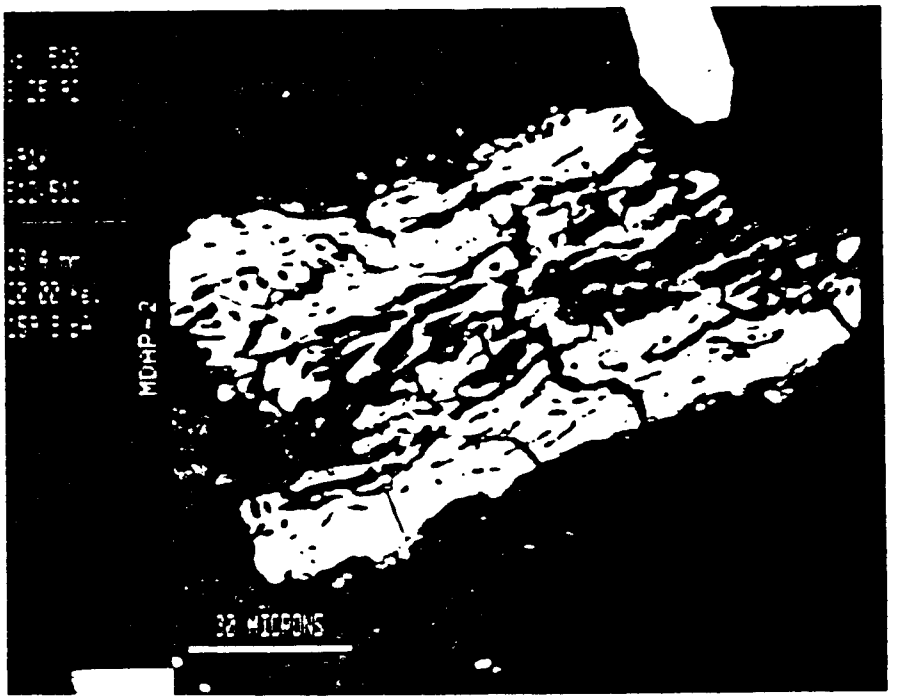

Conclusions

1. Soil samples from the barium nitrate storage area show a peak in barium concentration in soils 120 feet downslope. This could be explained by a slug input of barium into the channel.
2. Aluminum shows the same peak in concentration, indicating a correlation between aluminum and barium. This could be due to more aluminum oxides or a higher percentage of clay.
3. SEM images of BBG-4 and MDAP-2 show barium in three forms: With sulfate in barite crystals, as an oxide or carbonate within feldspar crystals and the pumice matrix, and as a barium compound adsorbed onto organic material.

CHAPTER 4
Field Screening for Barium using Laser-Induced Breakdown Spectroscopy

Introduction

Conventional elemental composition analysis of soils is accomplished using a variety of methods, including atomic emission spectroscopy (AES), atomic absorption spectrometry (AAS), x-ray fluorescence, and neutron activation analysis. Although these methods exhibit good detection limits and accuracy for most elements of interest, sample preparation and analysis can often be time consuming and the cost for analysis is often quite expensive. For the purposes of field monitoring contaminated sites, for instance determining a rough estimation of the spatial extent of contamination, or monitoring the efficiency of remediation processes, minimizing cost via rapid field analysis may be more important than the high accuracy and precision provided by conventional methods.

One method of elemental analysis of solids that requires little or no sample preparation and that is adaptable to remote analysis is the laser microprobe technique, also called laser-induced breakdown spectroscopy (LIBS). A laser pulse is focused to a sufficiently high irradiance to generate a microplasma which is used for spectrochemical analysis. Immediately following formation of the microplasma, the temperature and electron density can reach 25,000K and 10^{19} cm^{-3} (Radziemski et al., 1983). At these high temperatures, matter in the spark volume is vaporized, reduced to its atomic constituents, and then electronically excited (Radziemski et al., 1989). Emitted species in the spark are identified spectrally and temporally by resolving the spark light using a time-gated linear photodiode array.

Because the laser spark is a pulsed source, its excitation characteristics are a function of time. Within the first few hundred nanoseconds after spark formation, the spectrum is dominated by a spectrally broad background continuum due to bremsstrahlung radiation from electron-ion collisions. As the plasma cools, the intensities of ion lines and the background light decrease significantly due to a reduction of the temperature and electron density, and emission lines due to neutral elements and simple molecular species (such as CN) appear. (Radziemski et al., 1989).

Chromium Study

A previous study has been done with trace element detection using LIBS. This study, by Hans and Cremer (1992), focused on using LIBS to determine the concentrations of chromium, lead, and beryllium in soils. Detection limits of 2 ppm for chromium and lead and 0.1 ppm for beryllium were determined. For measurements using 100 sparks, accuracies were within 80% and precision was 20% or better for chromium detection. Effects of water, oil, and sample homogeneity on the analysis capabilities of the method were also studied. The presence of a significant amount of water within the soil (about 3.5 ml per 13 gm soil) gave a very weak signal, probably due to the large fraction of laser energy required to vaporize water from the sample which would ordinarily be used to vaporize the soil sample itself. The presence of oil in the soil (enough oil to thoroughly coat the soil particles) reduced the chromium signals by 37%. Sample homogeneity was examined by mixing clean soil with chromium contaminated samples made using solutions. The results indicate that the accuracy was reduced somewhat using these mixtures, but that it remained within the range (less than 20% difference) obtained with uniform samples.

Application of LIBS to barium

Developing LIBS to detect barium in soils in the field would be helpful in screening for soil contamination and determining the effectiveness of remediation efforts. The first step in developing LIBS for barium was finding a suitable element to ratio with the barium signal (see below). Silica was chosen to ratio with barium. Then suitable barium and silica emission spectra lines were found. Once it was determined that barium could indeed be detected with the LIBS instrument, development of the lab instrument to quantitatively determine barium concentrations in soils was undertaken. To develop the instrument quantitatively it was necessary to create an instrument calibration curve, determine instrument detection limits and precision, and find what physical factors such as soil moisture affect barium to silica ratios. Once it is shown that the lab instrument can be used to quantitatively detect barium in soils, then a field instrument can be developed.

Methods and Discussion

Apparatus

A schematic of the apparatus for performing laser spark analyses is shown in figure 4.1. The main components are the laser, a focusing lens, a fiber optic cable , a

Laser-Induced Breakdown Spectroscopy
-LIBS-

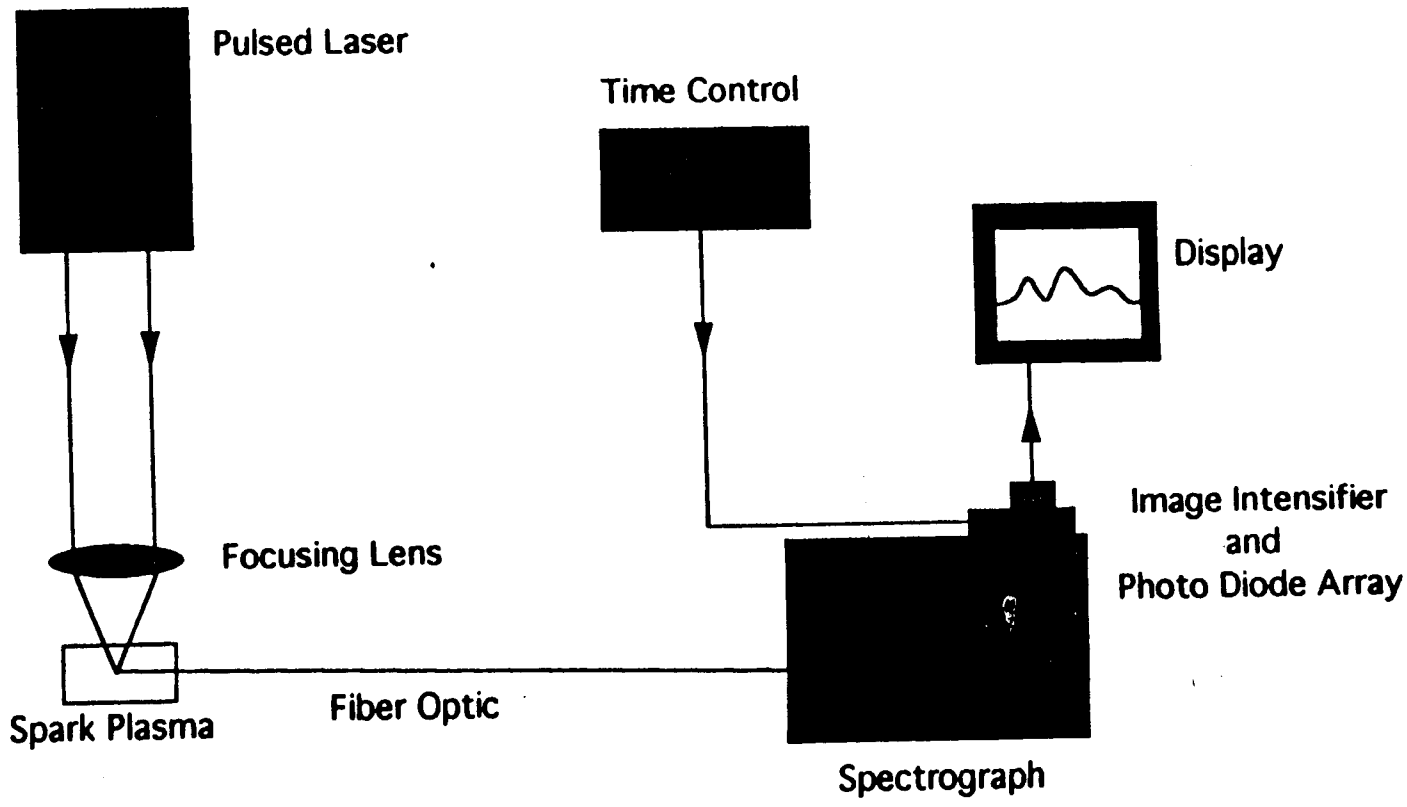

Figure 4.1: LIBS Apparatus Setup

spectrograph, a photodiode array detector, a time controller, and a computer for display and storage of spectra.

The laser used for laser spark analysis is a Q-switched Nd:YAG laser, Quanta-Ray DCR-11, with 10ns pulse width, 142-291 mJ pulse energy, and 1-10 Hz repetition rate.

The laser pulses are focused on the sample to form a spark using either a spherical or cylindrical lens. The laser spark produced using a glass spherical lens with a 50 mm focal length is about 0.1 mm in diameter, while the glass cylindrical lens with 150 mm focal length creates a long spark, 0.1 mm wide and 6 mm long . A much larger surface area of sample is analyzed using the long spark, giving better accuracy than the highly localized spark created by the spherical lens (see section).

A fiber optic cable is used to collect the spark light and direct it to the detection system. A fused silica, incoherent bundle fiber optic cable is used, and is 1 m long and 3 mm in diameter. Maximum light collection is critical, and is accomplished using the fiber optic because the fiber has a large acceptance angle. The fiber optic was positioned about 25 - 35 mms above the soil sample.

Spectral regions of the spark light are selected for analysis using an Instruments SA, model He-320, with 0.32 m focal length and gradations of 1200 or 2400 l/mm, and with slits 0.025-0.30 mm wide and 2 cm high. The spectrally resolved light is detected using a Tracor Northern time-gated linear photodiode array (DARSS System).

The method of time-resolving the emission signals depends on the detector. Time resolution with the photodiode array (PDA) is obtained by time-gating the voltage to the microchannel-plate image-intensifier in front of the array. In this way the gain of the PDA can be controlled by a factor of 10^6 and time resolution down to 5 nsec can be obtained (Radziemski et al., 1989).

Barium emission lines

The Hans study showed that during analysis, the distance between the soil surface and the laser spark changed due to pressure waves generated by the spark which moved the soil particles. Because of the change in power density on the soil as the surface-to-lens distance changed, significant shot-to-shot variations occurred in the emission intensities resulting in poor reproducibility, even if averaging over 100 sparks. These effects were minimized, however, by ratioing the chromium signal to the signal from an adjacent iron line. Shot-to-shot changes in the chromium and iron lines were similar so the ratio remained relatively constant. The assumption underlying the

use of line ratios was that iron is present throughout the soil at a fairly uniform concentration and that changes in excitation characteristics of the spark affected the iron and the chromium lines equally. While the iron may be uniformly present throughout a particular soil, the concentration of iron will not be constant throughout a variety of soil types. Therefore, for this barium study, it was opted not to use iron, but instead use silica to ratio to barium. While silica is certainly not constant throughout all soil types either, it is a significant component of most all soils and will be present in a more constant percentage than other elements.

The next step was to find a strong barium emission line with a close silica emission line so the two elements could be ratioed. A very strong barium emission line at 4554 nm was found, and a weak silica line was found at 5006 nm. No other stronger silica lines were located around the 4554 barium line. Because the barium and silica lines had very different energies, a dependence of laser energy with barium to silica ratio was found. Therefore we chose to use two other lines, a moderately strong barium line at 4130 nm and a silica line with similar intensity at 3905 nm (figure 4.2).

Analysis method

Samples were first analyzed using the spherical lens and the 4554 barium line, at a laser energy around 1.75 watts. Each measurement consisted of averaging the spectra from 100 laser sparks which at the laser pulse rate of 10 Hz corresponded to a measurement time of 10 seconds. The total counts under each emission peak was computed to be the emission signal. The trigger delay was 222 ns before the spectrograph was allowed to look at the spark, and after at 120 µsec the shutter to the spectrograph was turned off.

Spiked sand samples

In order to create the instrument calibration curve, samples of known barium concentration were needed. Since no standard soil samples were available, it was decided to spike soil samples with known amounts of barium chloride. Several different soil samples were preliminarily analyzed using LIBS and showed a significant barium signal. These uncontaminated soils were thought to have a significant amount of background barium, and thus were not useful for spiking because low barium concentration signals could not be separated from the background barium signal. Therefore a pure sand sample (which had a very low barium signal) was spiked and used for the calibration curve. Samples of 13 grams of

Figure 4.2: Spectrogram with Barium and Silica Lines

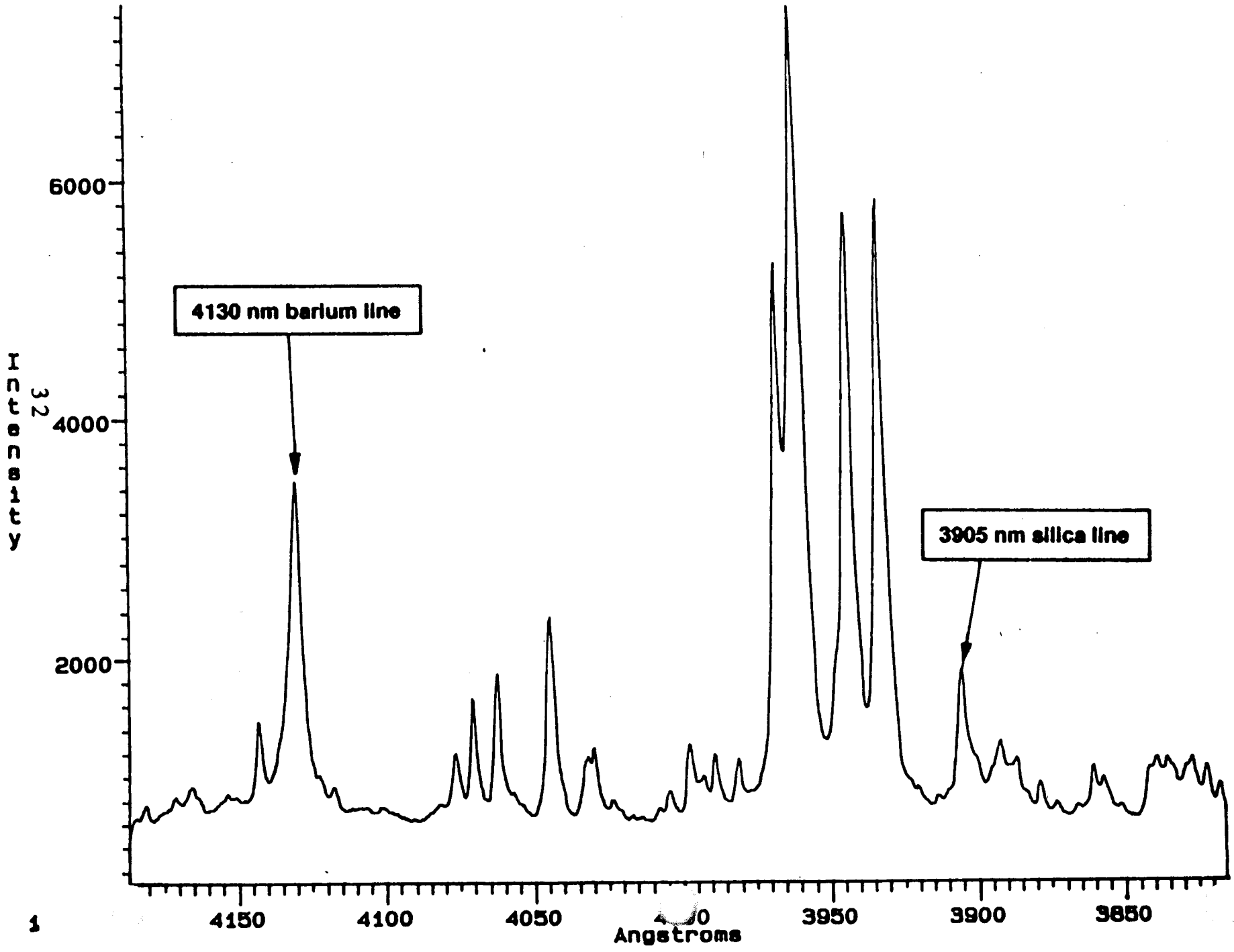

sand were spiked with 1.5 ml of varying concentrations of barium chloride solution. The solutions concentrations varied from 50 ppm up to 50,000 ppm, and a calibration curve was developed. Then the BBG and MDA-P soil samples (which have known barium concentrations due to XRF analysis) were run using LIBS to determine the accuracy of the calibration curve. The soil barium concentrations were calculated to be as much as 10 times lower than the actual barium level in the soil using LIBS.

There are several different explanations as to why the LIBS barium levels in the BBG and MDA-P soils were significantly lower than those found by XRF. First, the calibration curve may be incorrect. This, however, is doubtful since the spiked sand samples were run at least 5 times, each run showing the about the same barium to silica ratios and all showing the same similar trend in barium to silica ratio versus barium concentration.

Second, matrix effects may be affecting the intensity of the signal in the soil sample. The spiked sand samples are a well sorted sand with probable uniform silica content, and no silt or clay fractions. The soils, however, have significant silt and clay fractions in addition to sand. The high silica content of the spiked sand is very high (80 to 90%) whereas the silica content of the soils is lower (65 to 75%). Since barium is being ratioed to silica, the ratio in the soil will be higher (since silica is lower) than the sand. Thus the matrix effect produces the opposite effect from what is observed.

Third, the placement of the barium in the sand and soil samples may affect the intensity of the signals. The barium in the spiked sand samples will exist as a coating of barium chloride or some other barium compound on the surface of the sand grains. In the soils, however, barium exists as barite, other barium compounds, and barium adsorbed onto clay and organic particles. The energy required to free the barium in this form will be greater than a coating of barium on a sand particle. Therefore the intensity of the barium signal will be lower in the soil than in the sand.

Soil samples

Due to the problem with using spiked sand samples to determine the LIBS instrument calibration curve, it was decided to use the BBG and MDAP samples, whose concentrations are known via XRF, to create the calibration curve. Several attempts were made to find the average signal produced per soil sample, however precision errors were between 25 and 30%. The barium to silica ratio kept changing throughout a day's run, and ratios were not reproducible on subsequent days. The most likely correlation was with laser energy, which was thought to be constant. Laser energy versus time was measured (figure 4.3) and it was found that the laser energy

does indeed decrease throughout a day's run. The energy exhibits a large decrease in the first 15 to 20 minutes after being turned on, and then seems to level out to a relatively constant level, decreasing only about 0.2 watts per 15 minutes.

Since the laser creates a plasma at very high temperatures, laser energy should not affect the barium to silica ratios. However, the barium emission line chosen (4554 nm) is a very high energy line, whereas the silica emission line (5006 nm) is a low energy line. Since emission intensity is proportional to temperature (and to the Boltzman constant), any fluctuation in temperature due to laser energy changes will affect the intensity of the barium and silica emission lines. Because the barium and silica lines do not have similar energies, the intensities of the lines will not vary proportionally to each other given temperatures fluctuations. Thus, the barium to silica ratios will vary according to plasma temperatures, and thus laser energy. Therefore new barium and silica emission lines were chosen which have similar energies to avoid the dependence of barium/silica ratio to laser energy. The 4130 nm barium and 3905 nm silica lines were chosen, both of which have similar energies.

When the new silica lines were chosen, it was also opted to change the type of focusing lens used. Previously a spherical lens was used which creates a spark on the soil sample approximately 0.1 mm in diameter. The Hans study showed better precision when using a cylindrical lens which creates a long spark 0.1 mm wide and 6 mm long. The better precision is a function of more material being ablated per laser spark using the cylindrical lens, and decreasing the effect of inhomogeneity of chromium (or barium) distribution within the soil. The laser energy had to be increased using the cylindrical lens because the laser energy is dispersed over the larger area of the spark, compared to the spark created by the spherical lens.

With the new barium and silica emission lines and the cylindrical lens, a calibration curve was created using the BBG and MDA-P samples. This calibration curve is shown on figure 4.4. The calibration points are best interpolated using a second order polynomial function:

$$Y = -86x^2 + 2139x - 2520 \quad R=0.97$$

Table 4.1 shows the average barium/silica ratio with the sample barium concentration, along with the percent precision associated with each point. The highest precision error of these samples is 10.4%.

The accuracy of the calibration curve was preliminarily tested using the powdered BBG-1 soil sample used for XRF analysis, and also by using powdered XRF

standards. The powdered BBG-1 sample showed an average barium/silica ratio of 2.3599, compared to 2.5074 found with the soil sample, a difference of 5.9%. This precision is lower than the precision for BBG-1 soil sample (2.6%), probably due to the powdered nature of the BBG-1 XRF sample. As the laser spark hits the sample, a shock wave is formed, and the fine dust particles within the powder are thrown up into the air. This inhibits the fiber optic cable from obtaining a clear picture of the spark formed on the sample surface.

The powdered XRF standard results are shown in table 4.2. Generally the accuracy demonstrated for this calibration curve using the powdered XRF standards is very poor. Part of the problem could be the result of the dust in the air which obscures the fiber optic image, as described above, however it was shown above that this only affected the barium/silica ratio slightly. The accuracy of this calibration curve is questionable at this time. Other soil samples with known barium concentration (via XRF or some other analysis) would be required to further test the accuracy of this calibration curve.

TABLE 4.1

LIBS calibration curve points

Sample ID.	XRF Ba Conc. (ppm)	Ba/Si Ratio	% Precision
BBG-1	1741	2.5074	2.6
BBG-2	2361	2.9495	2.9
BBG-3	2639	2.8735	3.0
BBG-4	6224	4.1639	2.6
BBG-5	2814	3.0848	3.1
BBG-6	626	1.1988	3.5
MDAP-2	10026	9.7209	10.4

TABLE 4.2

XRF Powdered Standards

Sample ID	XRF BA Conc	LIBS Ba/Si Ratio	LIBS Ba Conc	% error
JB-1	490 ppm	1.3349	182 ppm	63
JB-2	208 ppm	1.2723	62 ppm	70
BIR-1	8 ppm	1.5744	635 ppm	99

Conclusions

1. The 4130 barium and 3905 silica lines give precise barium to silica ratios (as high as 10.4% relative deviation) without a dependence on laser energy.
2. Spiked barium sand and soil samples exhibit higher barium to silica ratios because the barium compound most likely exists as a coating on the sample, and is not adsorbed onto the clays and organic matter in the soil.
3. The instrument calibration curve is a second order polynomial:

   $Y = -86x^2 + 2139x - 2520 \quad R=0.97$

   The accuracy of the calibration curve is unknown at this time.

CHAPTER 5

Further Studies for Barium Transport Project

Although much has been learned about the transport of barium in soils over this summer's study, more questions have been raised than answered. There is still much to be done on this project to be able to characterize, with any certainty, the transport of barium within soils. Therefore, here are a few suggestions for further studies on the transport of barium.

Soil Samples

1. Characterize the BBG soil samples in detail to try to find a relationship between barium concentration to soil type. Analysis should include:
   a. mineralogy - types of clays present
   b. sand/silt/clay percentages
   c. organic matter content
   d. dry bulk density
   e. porosity
   f. soil pH
2. Determine a definite range of distribution coefficients for barium and a regular relationship between K_d and soil characteristics.
3. Develop a hydrodynamic model for barium transport within the soils at S-site.

LIBS

1. Determine the accuracy and the detection limits of the laboratory instrument. If these are within
2. Using the SEM determine the exact placement of barium chloride on spiked soil and sand samples to determine the exact cause of the high signals from spiked samples compared to "naturally" contaminated samples.
3. Determine the effects of soil moisture, inhomogeneous barium distribution, matrix effects, and organic matter content on barium signal.
4. Assess the pros and cons of using silica for a ratio to barium. Possibly find a more suitable element to ratio to the barium signal.

REFERENCES

Barr, M., June 1, 1992. Conference describing current barium studies at S-site.

Chang, R.. Chemistry, 2nd Edition. Randon House, Inc., New York, 1984.

Drever, J.I.. The Geochemistry of Natural Waters, 2nd Edition. Prentice-Hall, Inc., New Jersey, 1988.

Ferendaugh, W.R., Gladney, E.S., Brook. G.H.: 1979. Sigma Mesa Background Elemental Concentrations in Soil and Vegetation. LANL Pub. 11941-MS.

Gillham, R.W., Sharma, H.D., Reddy, M.R., Cooper, E.L., Cherry, J.A.: 1981. Barium and Radium Migration in Unconsolidated Canadian Geological Materials. Atomic Energy Control Board.

Han, M.Y., Cremers, D.A.: 1992. Rapid Determination of Metal Contaminants in Soils using the Laser Spark. Accepted to the International Journal of Environmental Analytical Chemistry.

ICAIR Life Systems, Inc.. The Drinking Water Criteria Document on Barium. Report prepared for Criteria and Standards Division, Office of Drinking Water, USEPA, 1990.

Kabata-Pendias, A., Pendias, H.. Trace Elements in Soils and Plants. CRC Press, Inc., Florida, 1984.

Multimedia Environmental Pollutant Assessment System (MEPAS), Constituent Data Base. USEPA, 1987.

Pidgeon, L.M.: 1984. Barium. In: Kirk-Othmer Encyclopedia of Chemical Technology, 2nd Edition, Volume 3. John Wiley and Sons, New York.

Radziemski, L.J., Cremers, D.A. Laser-Induced Plasmas and Applications. Marcel Dekker, Inc., New York, 1989.

Turner, A.: 1971. Environmental Studies at S-site. Water and Soil Analyses for RDX-HMX, Barium, TNT, and Boron. Summer study through GMX-3.

USEPA: 1984. Protecting the Nation's Groundwater from Contamination: Volume II. Report No. OTA-O-276.

Weast, R.C.. CRD Handbook of Chemistry and Physics. CRC Press, Inc., Florida, 1985

APPENDIX A
Field Soil Sampling

Soil samples were taken in late June and early July at S-site. Six samples from the barium nitrate storage/burial ground, two samples from MDA-P, and three samples from the hypalon pond were collected.

Barium storage/burial site

All of the storage ground samples were taken from a dry channel which runs through the storage area, downgradient from the area, and beside MDA-P (see attached polaroids of each sampling site). These samples were named BBG (for barium burial ground). Samples were taken for the purpose of determining the levels of barium coming from the storage area, and to determine how far the barium will travel down the most likely transport path, the stream bed. BBG-5 was taken beside MDA-P to determine if the landfill is contributing any barium contamination to this stream path, or if all barium in the stream is from the storage area. An upstream sample (BBG-6) was taken to determine background barium concentrations within the stream bed soils.

BBG-1

Sample was taken 6 feet from the 4th fence post with a heading of N17W. The area is a sediment trap within the dry drainage. Area is directly below the suspected BaNO3 storage area, and should have the highest barium concentrations of all the samples collected today. Sample taken was approximately 6 inches deep, and large pebbles and cobbles were avoided in sample taking.

BBG-2

Sample was taken 35 feet, bearing N23E from BBG-1. Sample also taken from a sediment trap in the dry stream, approximately 6 inches deep, avoiding large pebbles and cobbles. Sample location is approximately half way between storage area and dirt road.

BBG-3

Sample was taken 25 feet, bearing N33E from BBG-2. Sediment trap, approximately 6 inches deep, no pebbles or cobbles. Sample location is next to road (but looks undisturbed from road construction operations).

BBG-4

Sample taken 62 feet, bearing N9W from BBG-3. Sediment trap in same dry stream bed across the road, above MDA-P (to avoid contamination by MDA-P). Sample taken was approximately 6 inches deep.

BBG-5

Sample taken 64 feet, bearing N41W from BBG-4. Sediment trap approximately 1 1/2 feet from the main stream channel. Sample location is along side MDA-P, with what looks like a possible surface drainage channel coming from MDA-P from a small adit in the landfill. The adit has a wood retaining wall approximately 8 feet high, and is filled with concrete blocks, wood, and rebar. This adit is approximately 15 feet from the sample location. Sample taken was approximately 6 inches deep.

BBG-6

Background Sample. Sample taken upstream of the BaNO3 storage site from the same drainage as below. The soils are not exactly the same here as below; There are hardly any pebbles or cobbles, and much more vegetation covers this upstream location than downstream. Probably a process of no surface erosion above this site, whereas much surface erosion has occurred in the fenced-in storage area. Don states that the soil, however, looks disturbed. This must not have been too recently, however, since there is good vegetation covering the area. Sample is 95 feet, bearing N60E from the 2nd fence post from the SE corner of the fenced in area.

MDA-P site

Two samples were taken from a likely area of soil contamination within the landfill in order to get an idea of the levels of barium contamination we are dealing with in MDA-P. (See attached polaroids of each sampling site).

MDA-P-1

Sample was taken from a sediment trap on a small terrace below the top of the main landfill area. Cursory inspection of landfill material revealed 55 gallon drums, trash cans, pipes, paint cans, rebar, concrete, lots of glass. Sample was taken approximately 4 inches deep, taking care to avoid glass pieces. This sample failed the HE field screening test and could not be taken off site to be analyzed.

MDA-P-2

Sample was taken approximately 30 feet north of MDA-P-1 from a small sediment trap in another ledge. This ledge is the last ledge before the main drop into Water Canyon. Sample was 4 inches deep. Not as much refuse here, glass still present, but not as much.

<u>Hypalon pond site</u>

Three samples were taken from a dry channel below the hypalon pond. (No polaroids taken due to rain).

HYP-1

Sample was taken at the first major drop-off south of the hypalon pond, in a sediment trap.

HYP-2

Sample was taken 16 feet, 6 inches almost due south from HYP-1. Sample from a sediment trap in the dry channel.

HYP-3

Sample was taken 26 feet almost due south from HYP-2. Sample from a sediment trap in the dry channel.

BB6-5 6/26/92

BB6-6

C-LINE #52561
110 OR POLAROID
PRINTS

MDAP-1
6/26/92

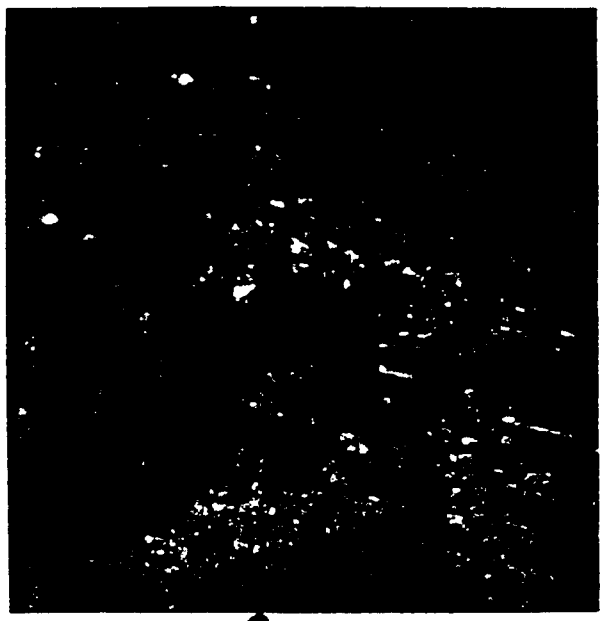

MDA-P 2

BB6-1 6/26/92
N-16-386

BB6-2 N-16-386
6/26/92

C-LINE #55531
110 OH POLAROID
PRINTS

BB6-3
6/26/92

BB6-4 6/26/92

CHARACTERISTICS OF BARIUM

A. Chemical

- silver-white alkaline earth metal
- similar properties to calcium except barium is more reactive and has a larger ionic radius
- seven naturally occurring isotopes
- melting point = 729°C; boiling point 1,640°C
- occurs in nature only in a combined state
- divalent and combines readily with oxygen, nitrogen, hydrogen, ammonia, water, halogens, and sulfides
- occurs most abundantly as sulfate, $BaSO_4$ (barite), and in smaller amounts as carbonate, $BaCO_3$ (witherite)
- as a metal oxidizes very easily and is decomposed by water or alcohol
- substitution for strontium and potassium ions common
- solubility
- low mobility in oxidizing and neutral conditions, acidic or alkaline pH
- very low mobility in reducing conditions
- found in solution as a free ion rather than hydrolysates or complex ions

B. Biological

- not an essential nutrient for most biological species
- as an environmental pollutant it is moderately toxic
- all barium compounds that are water soluble or acid soluble are poisonous
- toxic to humans chemically if taken into the body as a soluble salt (i.e. $BaCl_2$)
- causes serious deterioration to the heart's function and causes ventricular fibrillations
- chronic effects include bronchial irritation, degeneration of the CNS, and damage to the spleen, liver, and bone marrow
- insoluble barium (i.e. $BaSO_4$) is not harmful to humans and is used as an opaque solution in x-ray studies
- plants have been shown to accumulate barium from the soil
- food primary source of barium exposure to general population
- atmospheric barium emitted through industrial processes (refining and production of barium-based chemicals)

CHARACTERISTICS OF BARIUM (continued)

C. Regulatory Limits and Detection Limits
- USEPA drinking water standard = 1 mg/L
- Subpart S action level = 4000 ppm in soil; 100 ppm in water
- common detection limit in soil = 10 ppm; 1 ppm in water (dependent on analytical technique)

D. Hydrogeochemical
- concentration of sulfate in surface and groundwater likely control of barium
- distribution coefficient of barium

E. Existing barium data at S-site
- Turner study
- Barr study

Common barium compounds and their solubilities

Barium Compound	Solubility
Barium hexaboride (BaB_6)	Insoluble in cold water
Barium carbonate ($BaCO_3$)	0.002 g/100 ml @ 20°C
Barium chloride ($BaCl_2$)	37.5 g/100 ml @ 26°C
Barium hydroxide ($Ba(OH)_2$)	5.6 g/100 ml @ 15°C
Barium nitrate ($BaNO_3$)	8.7 g/100 ml @ 20°C
Barium oxide (BaO)	8.7 g/100 ml @ 20°C
Barium orthotriphosphate ($Ba_3(PO_4)_2$)	Insoluble
Other barium phosphates	Somewhat insoluble or decompose
Barium selenate ($BaSeO_4$)	0.0118 g/100 ml in cold water
Barium silicate ($BaSiO_2$) (metasilicate)	Insoluble in cold water
Barium sulfate ($BaSO_4$)	0.0002 g/100 ml @ 15°C

DISTRIBUTION COEFFICIENTS

Definition

A distribution coefficient (K_d) is a measure of the affinity of a solute for a solid phase. The higher the K_d value, the greater the tendency of the solute to be sorbed by the soil. K_d is expressed quantitatively as

$$K_d = \frac{\partial S}{\partial C}$$

$$S = \frac{\text{mass of chemical constituent adsorbed on the solid part of the porous medium}}{\text{unit mass solid}}$$

C = solute concentration in solution

Distribution coefficients for barium

Retardation equation

The distribution coefficient is important in determining the retardation of an element within a solid phase, as described by the Retardation Equation:

$$\frac{v}{v_c} = 1 + \frac{r_b}{n} \cdot K_d$$

v = average linear velocity of groundwater

v_c = velocity of the retarded constituent

r_b = dry bulk density of solid phase

n = porosity of solid phase

$\{1 + (r_b/n) \cdot K_d\}$ = Retardation Factor.

- dry bulk density (r_b) for unconsolidated sediments is typically around 2.65
- porosity (n) for unconsolidated sediments ranges from 0.2 to 0.4
- thus the (r_b/n) ratio range from 4 to 10 for unconsolidated sediments

For Kd = 1, for unconsolidated sediments,

$$\frac{v}{v_c} = (1 + \{4 \text{ to } 10\} \cdot 1) = 5 \text{ to } 11$$

So if an element has a K_d value of 1 in unconsolidated sediments, the solute will be retarded by a factor of 5 to 11. If Kd values are orders of magnitude larger than 1, the solute is essentially immobile.

Distribution coefficients for barium (MEPAS)

	< 10%	10 - 30%	> 30%
pH ≥ 9	530	2800	16000
pH 5 - 9	530	2800	16000
pH ≤ 5	53	280	1600

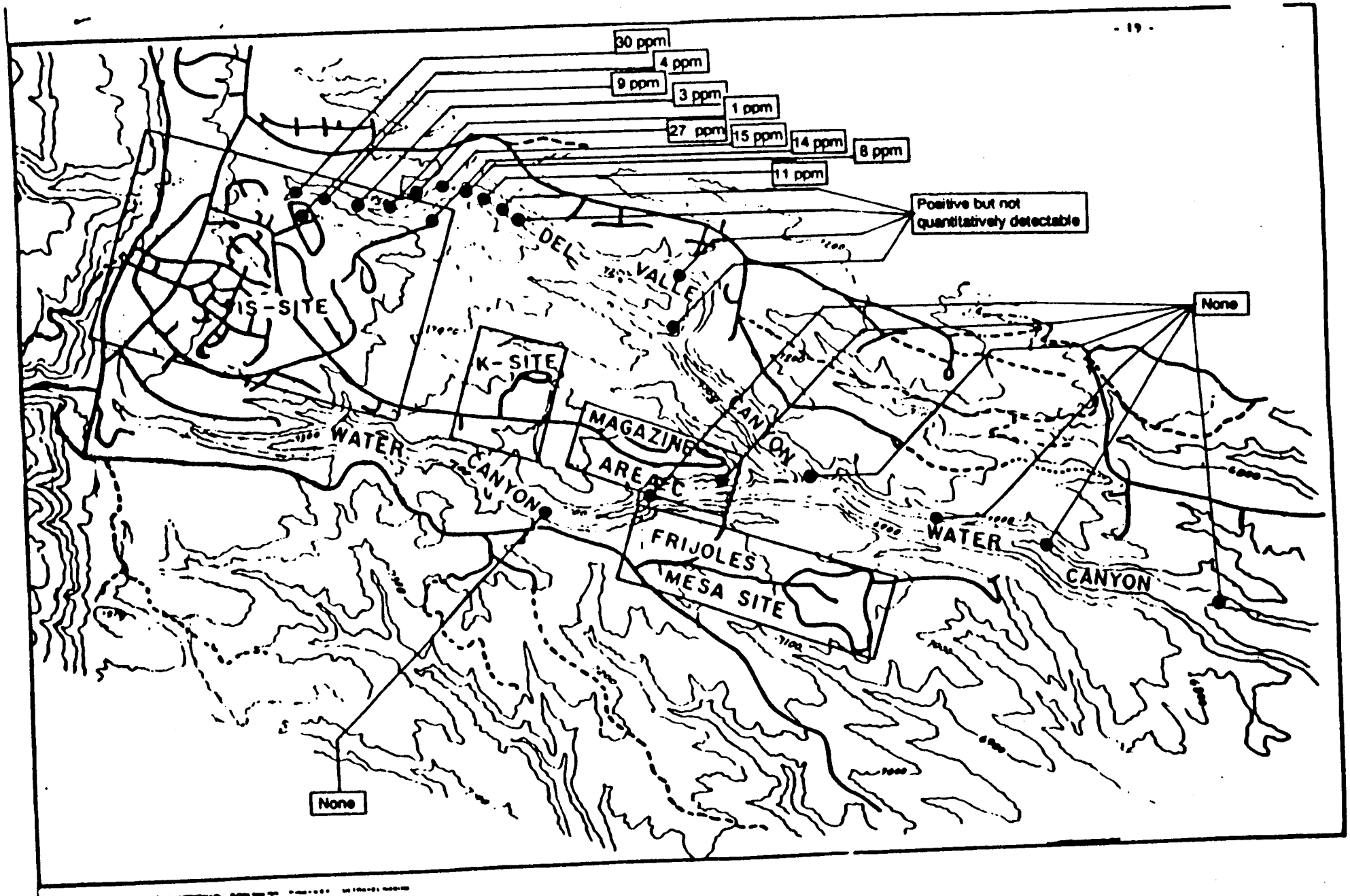

Figure 2.1: Sampling Locations in Turner Study

Barium concentrations in soil and water from Turner study

Sample Location	Ba Concentration
Water sample from settling tank behind Bldg. 260	4 ppm
Soil sample from the natural drainage area for the MDA-P burning pit	14 ppm
Water canyon	None
Along Del Valle Canyon:	
Water sample of surface drainage from Bldg. 260	30 ppm
Soil sample 400 yds down from Bldg. 260	9 ppm
Soil sample 100 yds down from previous	3 ppm
Water sample 100 yds down from previous	1 ppm
Water sample taken from point where drainage from MDA-P hits the canyon floor	27 ppm
Water sample taken 100 yds down from previous	15 ppm
Water sample taken 100 yds down from previous	8 ppm
Water sample taken 100 yds down from previous (water in pool)	11 ppm
Soil samples downstream from previous to the confluence of Del Valle and Water Canyon	Positive but not quantitatively detectable

Barium concentrations in soil and water from Barr study

Sample Location	Ba Concentration
Pond behind Bldg. 260	5000 ppm (with a high amount of HE)
Downstream of this pond 135 ft.	3500 ppm
210 ft. downstream - natural ponding area	6500 ppm
Area P burning ground (above)	1400 ppm
Area P burning ground (below)	1400 ppm

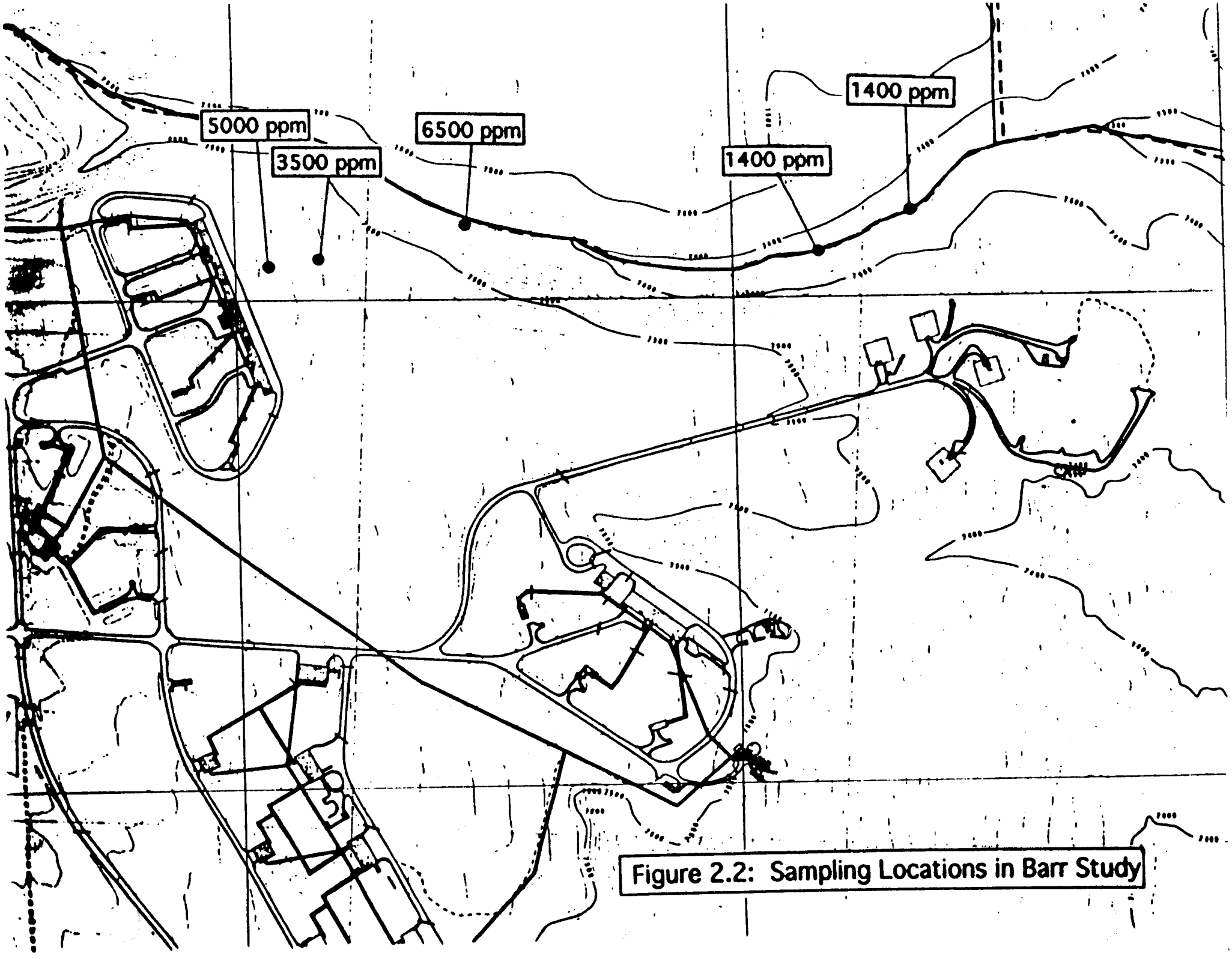

Figure 2.2: Sampling Locations in Barr Study

BARIUM IN SEDIMENTS
XRF AND SEM RESULTS

A. Soil Sampling
- soil samples taken from three locations at S-site, all suspected to have high barium and low HE concentrations

B. Soil Sampling Results
- soil samples analyzed by X-ray Fluorescence (XRF), using pellets made of a 50/50 ratio of soil sample to lithium tetraborate binder
- linear or exponential decrease in barium concentration from the source expected
- BBG samples show a peak concentration 120 feet downslope from the source
- two possible explanations for this trend:
  1) barium concentration is a function of clay, aluminum and iron oxide, or organic matter content in the soil
  2) slug input of barium

C. Scanning Electron Microscope
- barium was found in three different forms throughout the two slides:
  1) with sulfur in barite crystals
  2) as an oxide or carbonate within feldspar crystals and the pumice matrix
  3) as a barium compound adsorbed onto organic material

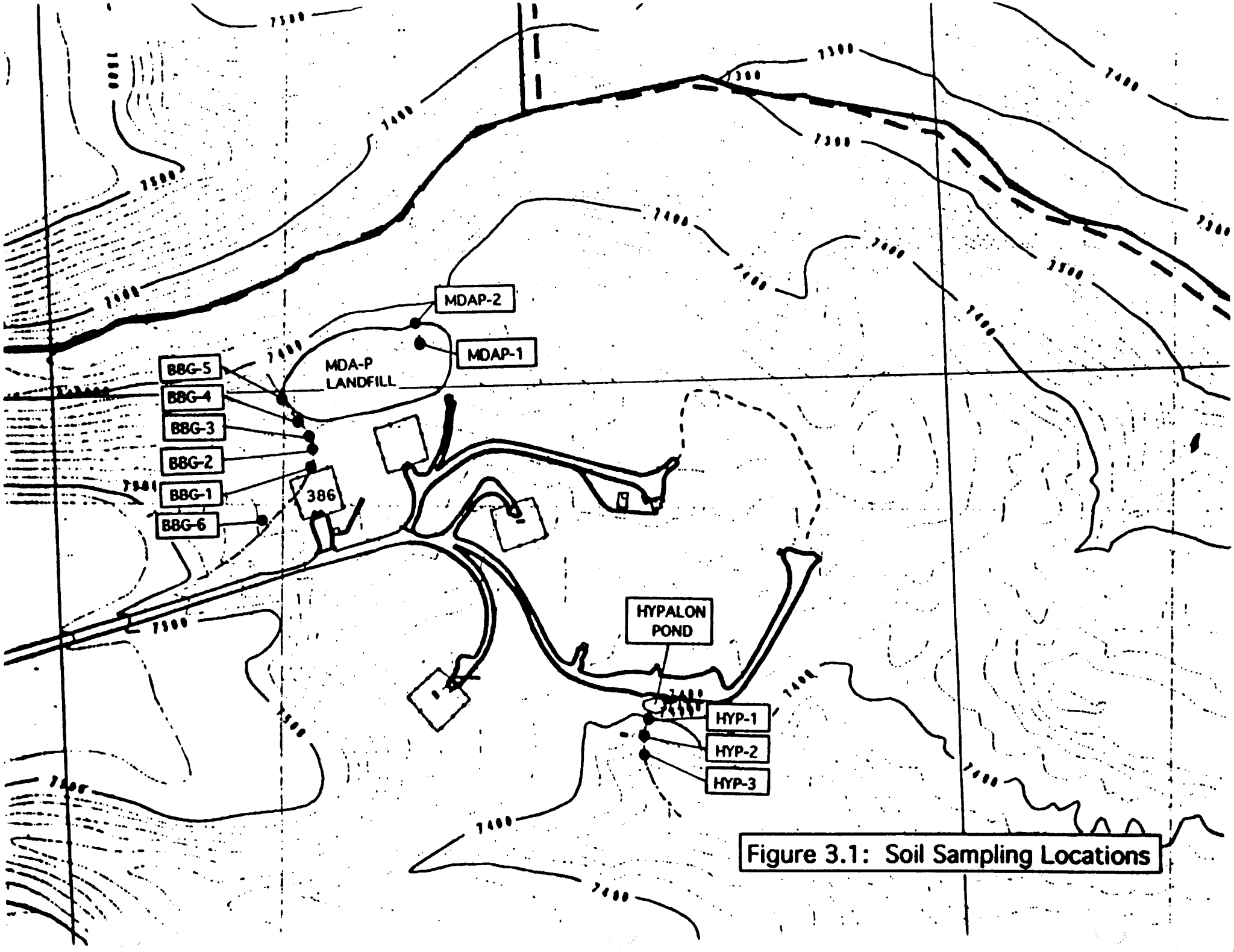

Figure 3.1: Soil Sampling Locations

TABLE 3.1

Soil Sampling Results

Sample	Na_2O %	MgO %	Al_2O_3 %	SiO_2 %	P_2O_5 %	K_2O %	CaO %	TiO_2 %	MnO %	Fe_2O_3 %
BBG-1	4.69	0.36	12.90	72.53	0.02	3.60	0.81	0.40	0.07	2.67
BBG-2	4.70	0.37	13.28	66.61	0.01	3.84	0.73	0.60	0.09	3.79
BBG-3	4.44	0.35	13.41	70.03	0.03	3.92	0.71	0.36	0.07	2.76
BBG-4	4.32	0.40	13.91	[illegible]	0.03	4.09	0.65	0.41	0.06	2.94
BBG-5	4.55	0.37	13.61	70.17	0.03	3.84	0.71	0.37	0.04	2.73
BBG-6	3.23	0.44	12.17	71.30	0.03	3.48	0.84	0.44	0.04	2.60
MDA-P-2	4.07	0.30	12.78	[illegible]	0.05	4.26	0.60	0.30	0.04	2.33
HYP-1	3.28	0.32	10.50	76.79	0.04	3.33	0.80	0.31	0.06	2.32
HYP-2	4.09	0.39	11.90	74.51	0.05	3.40	0.88	0.31	0.06	2.60
HYP-3	4.39	0.42	13.51	70.14	0.05	4.11	1.24	0.30	0.07	2.58

Sample	V ppm	Cr ppm	Ni ppm	Zn ppm	Rb ppm	Sr ppm	Y ppm	Zr ppm	Nb ppm	Ba ppm
BBG-1	40	8	15	167	56	152	16	373	34	1750
BBG-2	47	10	16	102	61	142	17	534	38	2351
BBG-3	43	8	16	70	71	135	19	320	38	2658
BBG-4	42	7	16	61	88	128	31	412	40	6253
BBG-5	44	8	14	58	73	129	26	326	37	2823
BBG-6	42	14	13	39	93	132	31	406	41	620
MDA-P-2	41	3	19	50	98	134	32	324	49	10026
HYP-1	39	7	16	61	64	143	19	268	32	1430
HYP-2	38	6	14	73	78	137	23	275	38	941
HYP-3	36	7	16	73	103	130	30	304	44	1100

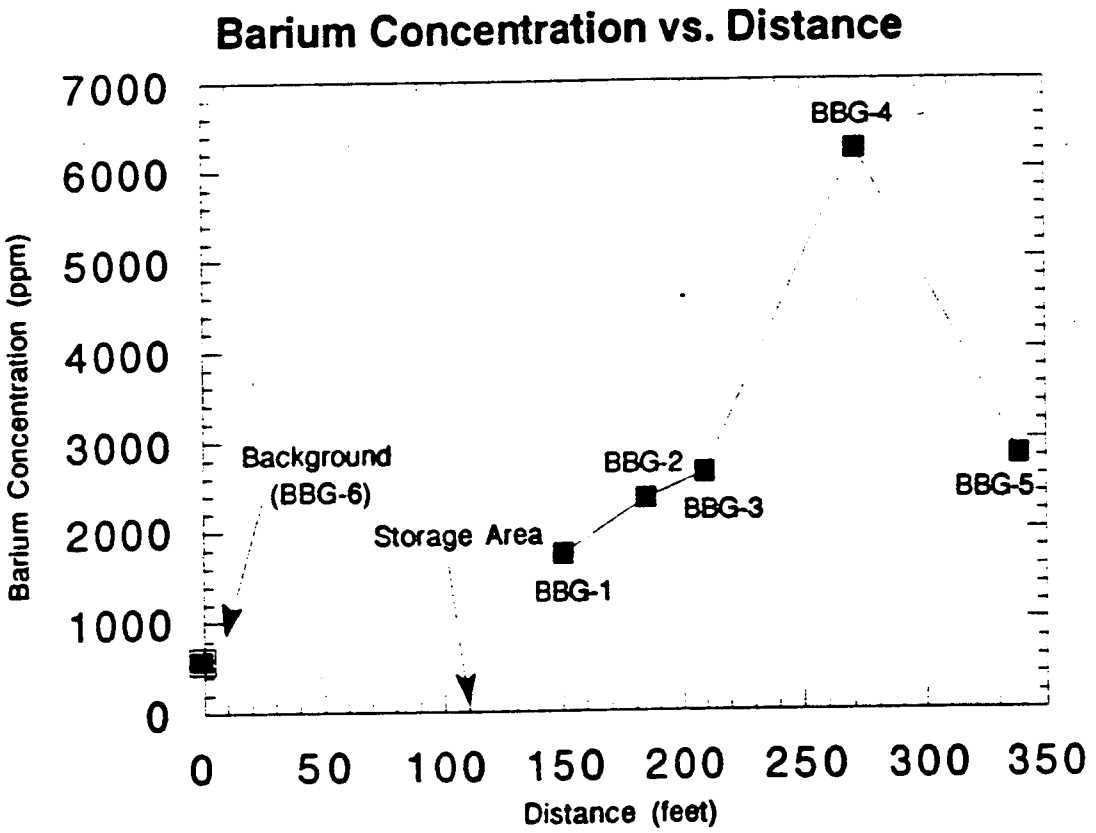
Barium Concentration vs. Distance
Barium Concentration (ppm)
7000
6000
5000
4000
3000
2000
1000
0
0
50
100
150
200
250
300
350
Distance (feet)
BBG-4
Background
(BBG-6)
BBG-2
BBG-3
BBG-5
Storage Area
BBG-1

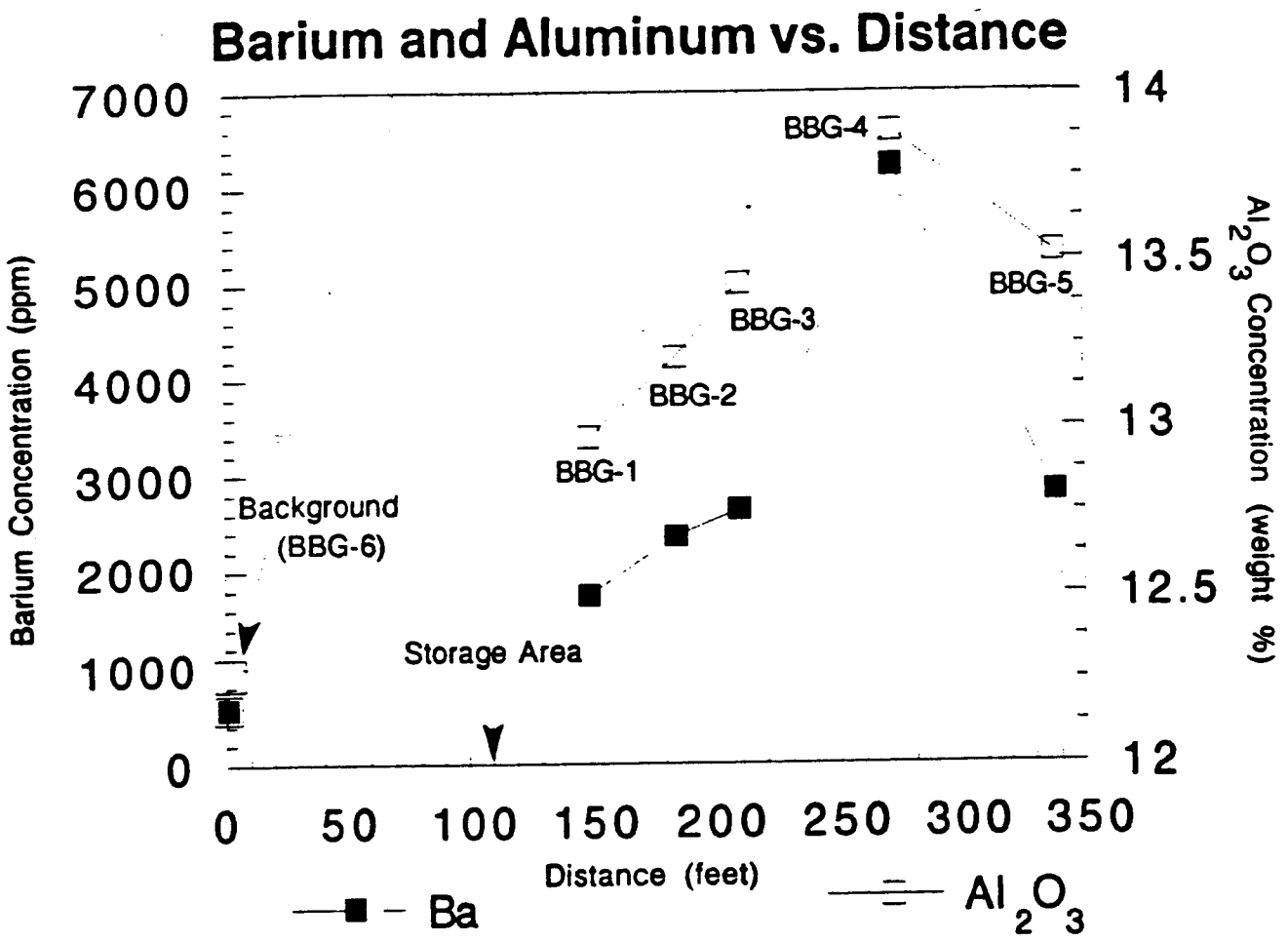
Barium and Aluminum vs. Distance
Barium Concentration (ppm)
7000
6000
5000
4000
3000
2000
1000
0
14
13.5
13
12.5
12
Al_2O_3 Concentration (weight %)
BBG-4
BBG-5
BBG-3
BBG-2
BBG-1
Background
(BBG-6)
Storage Area
0
50
100
150
200
250
300
350
Distance (feet)
Ba
Al_2O_3

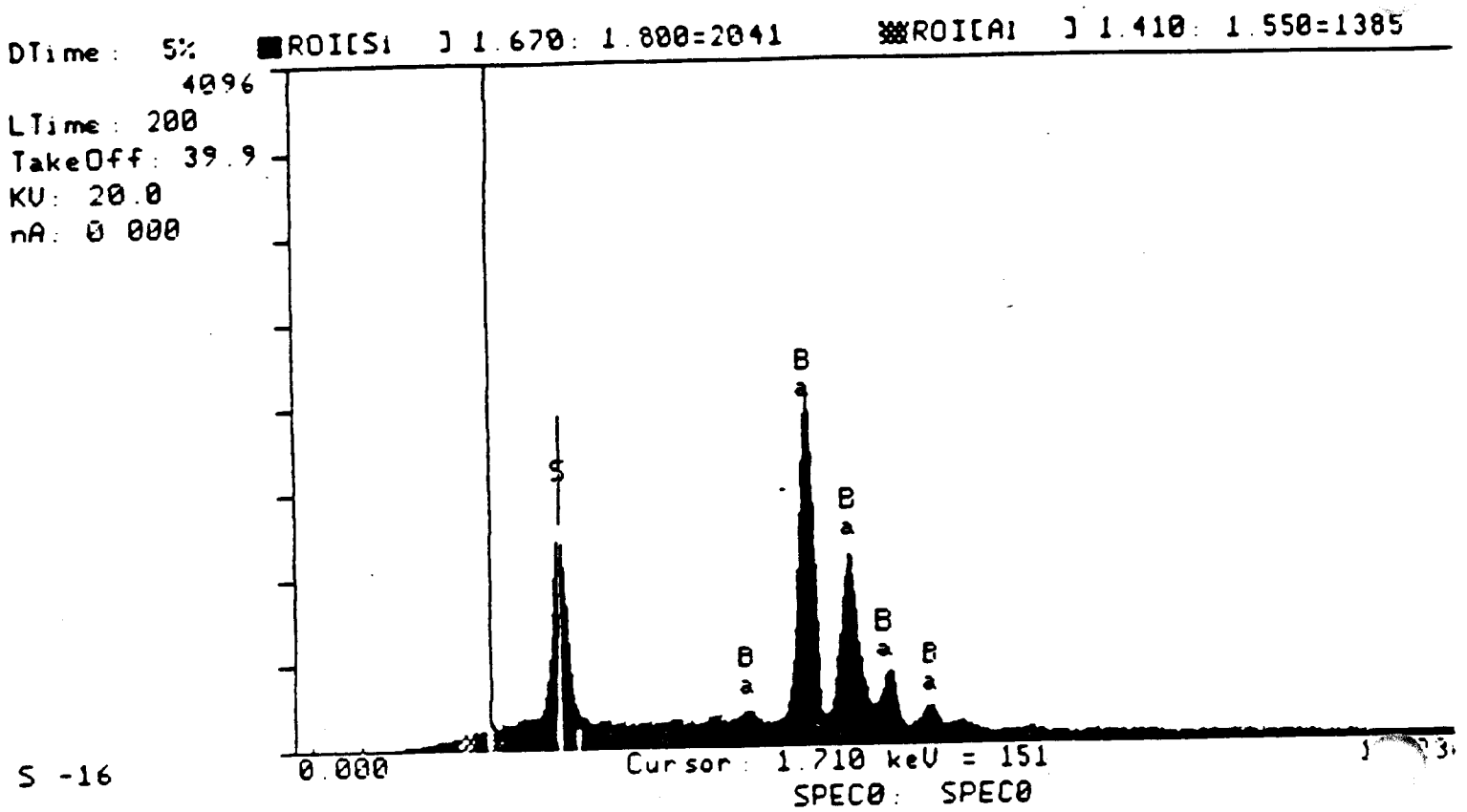
DTime : 5%
ROI[S]] 1.670 : 1.800=2041
ROI[A]] 1.410 : 1.550=1385
4096
LTime : 200
TakeOff : 39.9
KV : 20.0
nA : 0.000
S
B a
B a
B a
B a
B a
0.000
Cursor : 1.710 keV = 151
SPEC0 : SPEC0

S -16

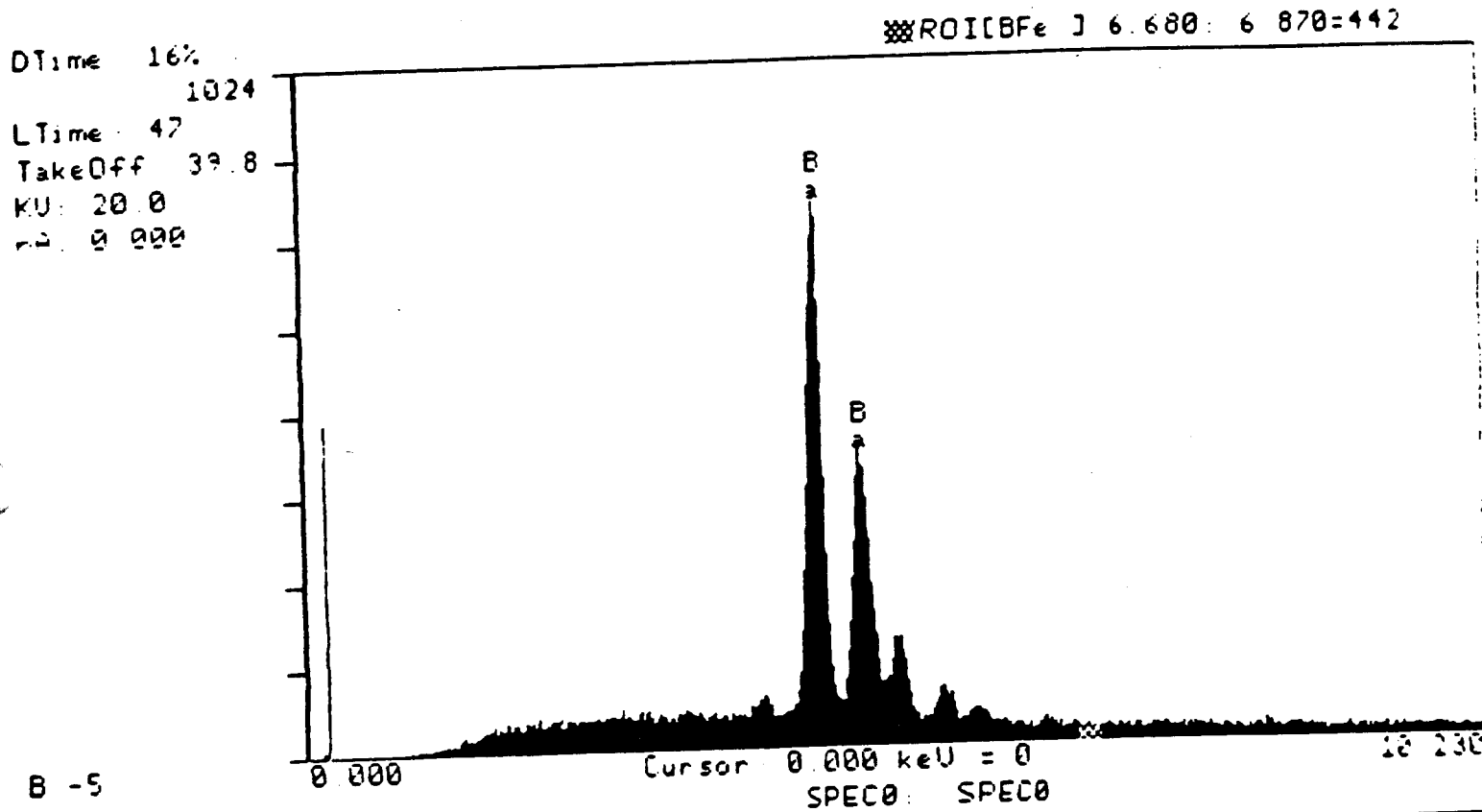
ROI[BFe] 6.680: 6 870=442
DTime 16%
1024
LTime 47
TakeOff 39.8
KV: 20.0
0 000
B
a
B
a
0 000
Cursor 0.000 keV = 0
SPEC0: SPEC0

B -5

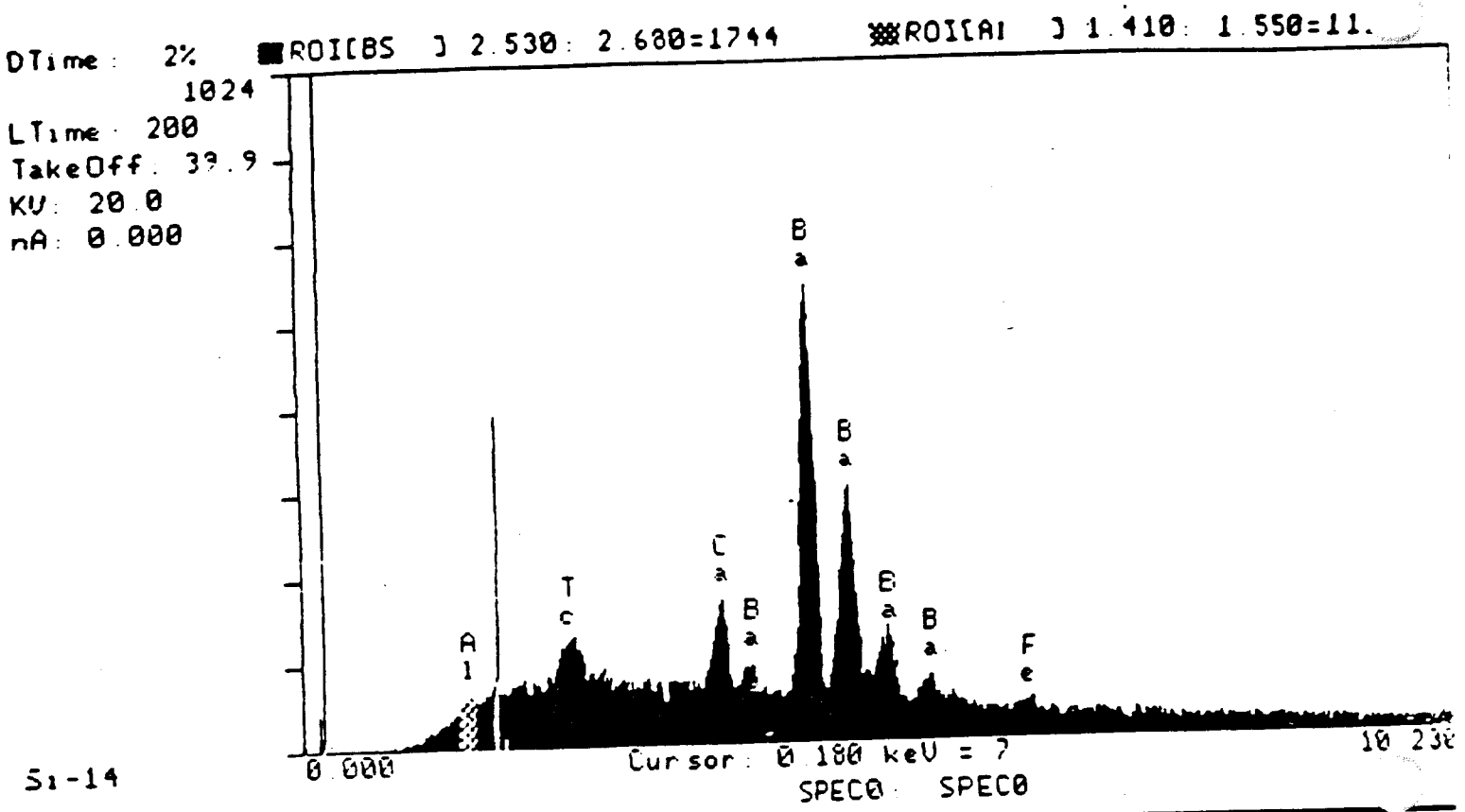
DTime : 2%
ROI[BS] 2.530 : 2.680=1744
ROI[Al] 1.410 : 1.550=11.
1024
LTime : 200
TakeOff. 39.9
KV : 20.0
nA : 0.000
Al
Tc
Ca
Ba
Ba
Ba
Ba
Ba
Fe
0.000
Cursor : 0.180 keV = 7
SPEC0 : SPEC0
10.230

Si-14

FIELD SCREENING FOR BARIUM USING LASER-INDUCED BREAKDOWN SPECTROSCOPY (LIBS)

A. What is LIBS?

- a laser pulse which is focused to a sufficiently high irradiance to generate a microplasma which is used for spectrochemical analysis
- following formation of microplasma the temperature can reach 25,000K
- matter in the spark volume is vaporized, reduced to its atomic constituents, and then electronically excited
- emitting species in the spark are identified spectrally and temporally by resolving the spark light using a time-gated linear photodiode array.

B. LIBS apparatus

- main components are the laser, a focusing lens, a fiber optic cable, a spectrograph, a photodiode array detector, a time controller, and a computer for display and storage of spectra

C. Application of LIBS to barium

- development of a field LIBS instrument for detecting barium in soils
  1) screen for soil contamination
  2) assess the effectiveness of remediation efforts
- chromium field LIBS instrument
  1) remote soil/rock analysis

D. Calibration curve

- began by using the 4554 nm barium emission line and the 5006 nm silica emission line
- found a dependence of laser energy to barium/silica ratio for these two lines
- now using the 4130 nm barium line and the 3905 nm silica line
- no dependence of barium/silica ratio using these two lines
- spiked soils versus contaminated soils
- precision error 13% at most
- accuracy undetermined

XRF Ba CONCENTRATION VS. LIBS Ba/Si RATIO

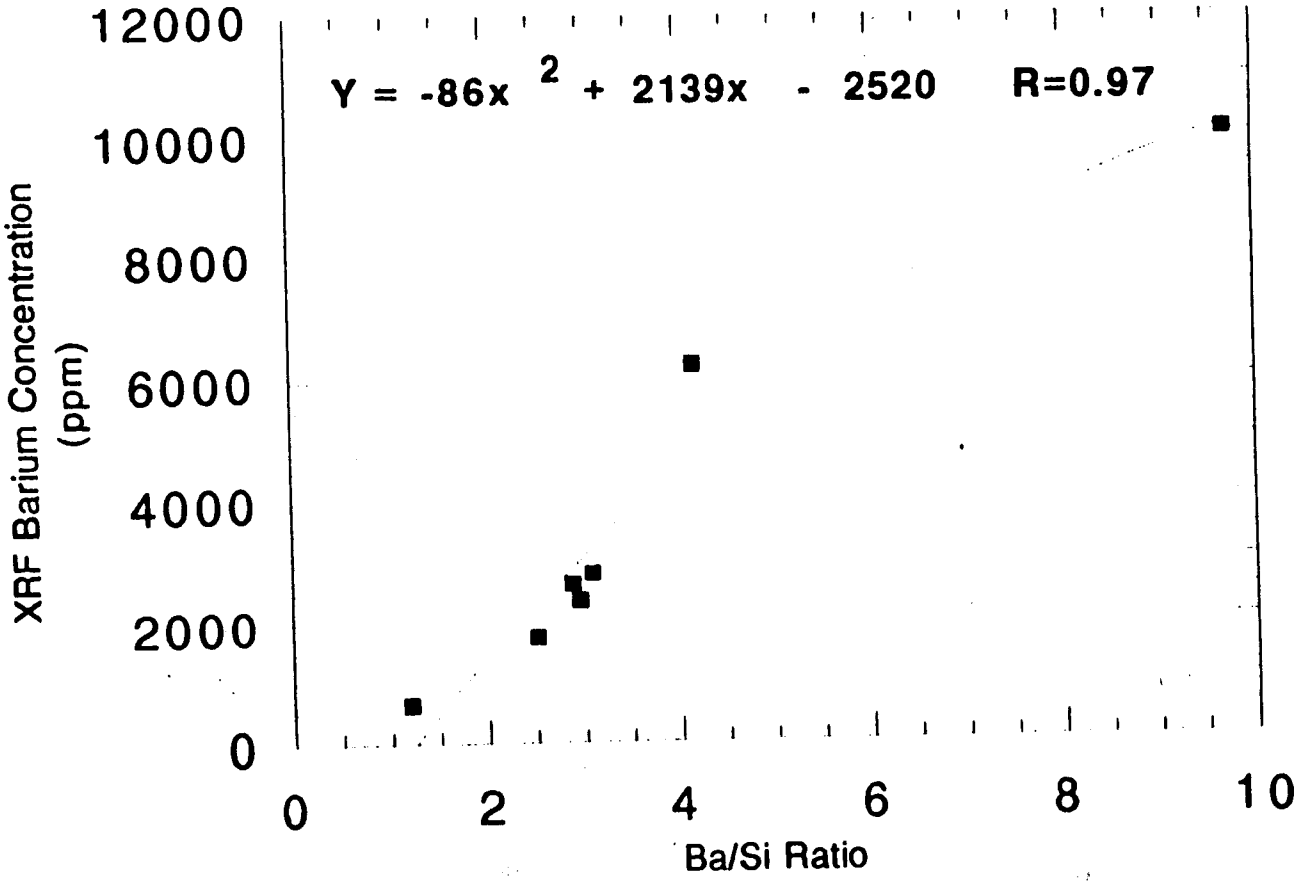

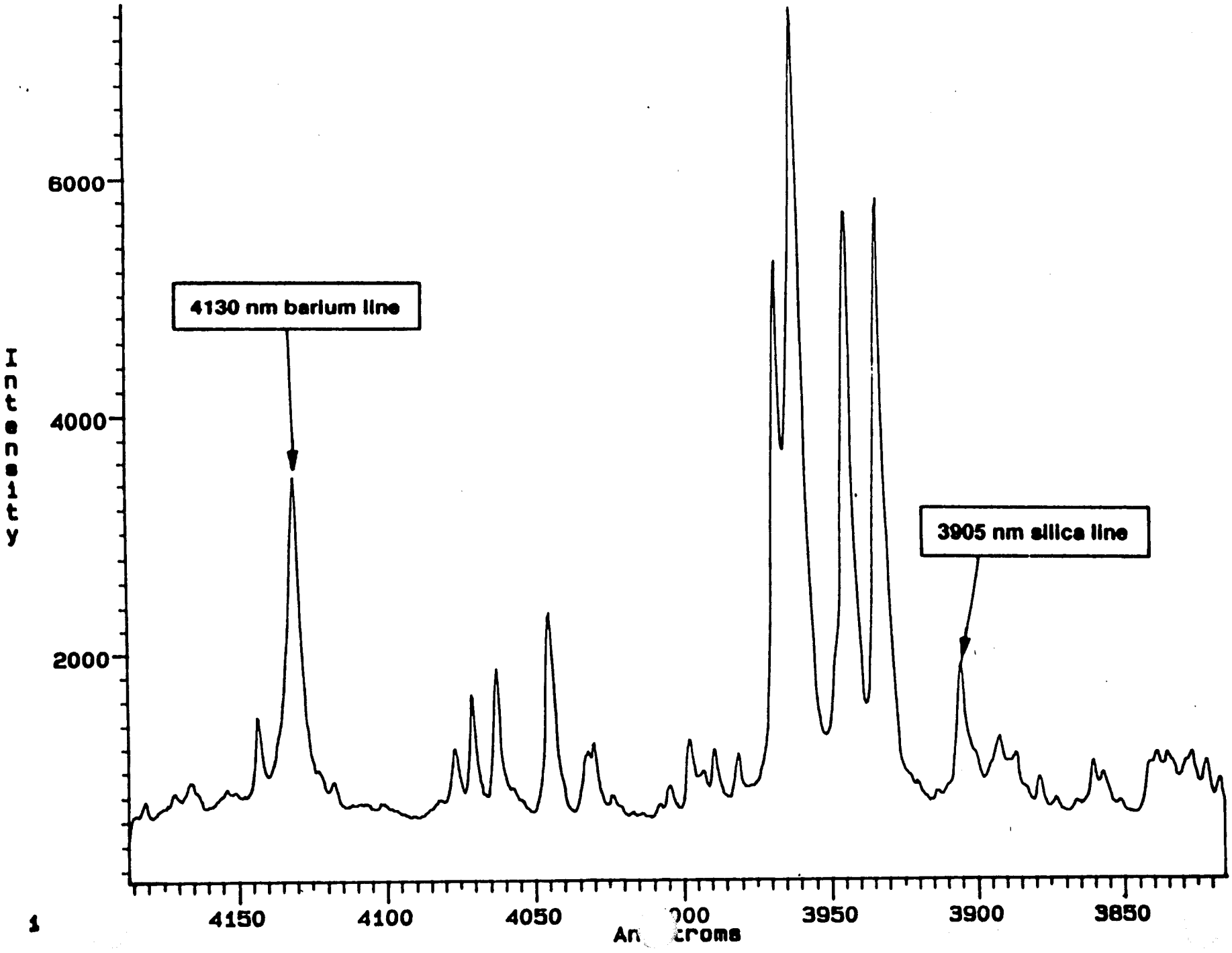
4130 nm barium line
3905 nm silica line
Intensity
6000
4000
2000
4150
4100
4050
3950
3900
3850
Angstroms

1

FURTHER STUDIES

A. Soil samples

- characterize BBG soil samples in detail to try to find a relationship between barium concentration soil type. Analysis should include:
  1) mineralogy - types of clay present
  2) sand/silt/clay percentages
  3) organic matter content
  4) dry bulk density
  5) porosity
  6) soil pH
- determine a definite range of distribution coefficients for barium and a regular relationship between Kd and soil characteristics
- develop a hydrodynamic model for barium transport within the soils at S-site

B. LIBS

- determine accuracy and detection limits of LIBS
- determine effects of soil moisture, inhomogeneous barium distribution, matrix effects, and organic matter content effects
- develop a field LIBS instrument for barium detection